LU TP 20-26
June 2020

The two-Higgs-doublet model as an explanation for the muon $(g-2)$ discrepancy

Zenny Wettersten

Department of Astronomy and Theoretical Physics, Lund University

Bachelor thesis supervised by Johan Rathsman

LUND
UNIVERSITY

Abstract

The general $\mathbb{Z}_2$-violating two-Higgs-doublet model (2HDM) is analysed as an explanation for the discrepancy between Standard Model predictions and experimental measurements of the muon anomalous magnetic dipole moment Δa_μ, with the condition that it does not provide an electron electric dipole moment $|d_e|$ larger than experimental bounds. Several point studies of individual 2HDM parameter space points are made to show large-scale cancellation among Barr-Zee 2-loop contributions to $|d_e|$ at large Yukawa lepton sector magnitudes, as well as an approximately linear growth of total a_μ contribution when those magnitudes are rescaled by a common factor, reaching the same order as Δa_μ. These point studies show that diagonally enhanced Yukawa couplings in the 2HDM could be an explanation for Δa_μ without violating experimental bounds on $|d_e|$.

Populärvetenskaplig beskrivning

Standardmodellen (SM) är det närmaste vi kommit en *theory of everything*. Den beskriver individuella partikelinteraktioner perfekt, gjorde vid dess formulering nya förutsägelser och har konsekvent visats ha rätt.

Den är även usel.

Trots att SM perfekt beskriver individuella partikelinteraktioner så stämmer modellens universella förutsägelser inte överens med verkligheten. Den kan inte förklara varför det finns mer materia än antimateria och den är oförenlig med Einsteins allmänna relativitetsteori. Av denna anledning studerar teoretiska partikelfysiker så kallade *bortom SM-modeller*, såsom två-Higgs-dublett-modellen (2HDM).

Säg att du är hemma och lagar tomatsås. Du smakar på såsen: Den är god, men den kunde ha varit bättre. Hur reagerar du? Din omedelbara reaktion hade antagligen inte varit att hälla såsen i vasken och börja om från början, utan du skulle helt enkelt krydda till den. Det är vad 2HDM är för SM — en *minimal förlängning*, där en lägger till ett extra fält med samma struktur som det väletablerade Higgsfältet som redan är en del av SM.

Men varför ett Higgsfält? Jo, som namnet minimal förlängning föreslår är Higgsfältet och dess tillhörande Higgsboson SMs enklaste delar. Det är ett *skalärfält*, till skillnad från de andra, vilka är *vektorfält* — fysikspråk, vilket betyder att när det gäller ordspråket, "En bild säger mer än tusen ord", är Higgsfältet ett ord medan de andra fälten är bilder. Fast orden är i det här fallet siffror. Andra fält rymmer massvis med information, men Higgsfältet berättar bara om en partikels massa och position.

Genom att lägga till ett extra Higgsfält får vi då nya *interaktionstermer*, vilket också är fysikspråk och betyder 'sätt olika partiklar kan göra saker med varandra'. SMs Higgsfält har kopplingar till elektronfältet och genom att *interagera* med Higgsfältet blir elektronerna massiva. Å andra sidan har Higgsfältet ingen koppling till fotonfältet, så fotonerna förblir masslösa.

När vi väl gjort matten så ser vi att tillskottet av ett extra Higgsfält leder till interaktionstermer som tillåter $\mathcal{CP}$-brytande interaktioner. Kort och gott hänvisar $\mathcal{CP}$-brott till mekanismer som kan skapa olika mängder materia och antimateria, så 2HDM skulle möjligtvis kunna lösa motsägelser angående universums utveckling.

Dessutom är 2HDM en nödvändig del av flera mer avancerade bortom SM-modeller, såsom supersymmetri eller supersträngteori, vilka kräver att olika sorters partiklar får massa från olika Higgsfält. Dessa kan ses som nya, mer avancerade recept du kan ta dig an när du bemästrat tomatsåsen.

2HDM är för SM vad lite extra krydda är för matlagning: Det räddar inte en fasansfull måltid, men det kan ge något gott, det där lilla extra. Modellen kan även bana vägen för mer innovativa recept. Innan en prövar något helt nytt är det dock vettigt att ta sig så långt som möjligt med det som finns till hands — varför gå till affären när du inte använt alla ingredienser i skafferiet? Därför testar vi 2HDMs duglighet: I hopp om att lösa problemen partikelfysiken står inför idag och sedan kunna hitta nya recept att testa framöver.

Contents

1 Introduction

With the observation of a 125 GeV scalar particle in 2012 [1, 2] which has not shown any deviation from the Higgs boson [3], the Standard Model of particle physics (SM) is complete [4]. Almost fifty years after the initial predictions of the scalar sector [5–7], the final piece of the SM was found.

Nevertheless, the SM has issues [8–11]. The full extent of these problems will not be detailed here, but one example is the baryon asymmetry of the universe [12] which necessitates e.g. extra sources of $\mathcal{CP}$-symmetry violation. There is a need for beyond the SM (BSM) physics. Although there are studies made into theories which would overthrow the current paradigms of particle physics, such as M-theory (a unification of the five lowest-dimensional supersymmetric string theories, seeking to unify quantum field theory and general relativity [13]), it is often simpler to work with so-called minimal extensions to the SM. Minimal BSM models, as the name suggests, make only minor additions to the SM and analyse those in the hopes that they might explain some failures of the SM.

One such minimal BSM extension is the Two-Higgs-Doublet Model (2HDM). Whereas the SM assumes the most basic possible structure for the scalar sector, a single $SU(2)$ doublet, the 2HDM extends this sector by adding another $SU(2)$ doublet of identical structure to the one in the SM [14]. Adding only a doublet is an arbitrary decision, and there is an infinite set of more complicated options [14], but the restriction to the single doublet addition lends itself to simplicity not offered by the more complex alternatives.

The 2HDM has the possibility for $\mathcal{CP}$-violation, which could help explain the previously mentioned baryon asymmetry [15]. Additional scalar doublets are also necessary in minimal supersymmetric theories [16]. Despite lacking any experimental evidence, supersymmetry remains a dream of large parts of the physics community, as it would provide an elegant solution to several of the issues of the SM [17]. Extra scalar doublets also appear, for example, in axion models [18], which try to explain the absence of $\mathcal{CP}$-violation in the strong interaction.

In addition to the far-ranging theoretical implications of the 2HDM, it would also contribute to the anomalous magnetic moments of leptons, such as the muon anomalous magnetic moment $\left(\frac{1}{2}(g-2)_\mu = a_\mu\right)$ [19]. The discrepancy between current experimental measurements of a_μ and the SM prediction, Δa_μ, is 2.68×10^{-9} or three and a half sigma [20], which M. Davier et al. [21] describe as "an interesting but not conclusive discrepancy". Although inconclusive, this discrepancy does provide a benchmark for 2HDMs, as they could serve to explain it should it remain with future, more sensitive measurements. However, any $\mathcal{CP}$-violating phase would also contribute to the electric dipole moment of the electron (d_e) [22], which has an experimental bound of $|d_e| < 1.1 \times 10^{-29}$ e cm [23]. It is not atypical for a $\mathcal{CP}$-violating 2HDM to surpass this limit by several orders of magnitude.

This thesis analyses the parameter space of the 2HDM based on first and second order $|d_e|$ and a_μ contributions to test whether a 2HDM could simultaneously give Δa_μ on the order of the one seen in current experimental data, while giving rise to a $|d_e|$ within experimental bounds. Previous studies into this have put emphasis on softly broken $\mathbb{Z}_2$ symmetries — see Section 2.4 for details. More general cases are treated here, such as

2HDMs with softly $\mathbb{Z}_2$-violating potentials but generally aligned Yukawa sectors, softly $\mathbb{Z}_2$-violating potentials with undiagonalisable Yukawa sectors, and 2HDMs with hard $\mathbb{Z}_2$-violating potentials and undiagonalisable Yukawa sectors. Regions of cancellation among the 2-loop d_e contributions are shown to exist at individual magnitude points for all regions, and for extended intervals of the Yukawa lepton sector magnitude in the hard $\mathbb{Z}_2$-violating potential case.

This thesis is divided into five main sections, starting with this introduction. Sections 2 and 3 detail the 2HDM, the former with regards to its formulation and previous studies into the subject as well as some details on $|d_e|$ and a_μ, and the latter with regards to its implementation for the purposes of this project, as well as describing the more practical software developments performed. Section 4 describes and showcases the results of the point studies performed in analysing a_μ and $|d_e|$ contributions of generalised 2HDMs. These results are discussed more extensively in Section 5, which is the conclusion of this thesis. Along with the main text, there are also three appendices: Appendix A is a short summary of the work towards attaining an analytic expression for the generalised 1-loop contributions to a_μ and $|d_e|$, Appendix B is an instruction manual for the `2HDME` extensions developed for this project, and Appendix C contains any extra figures not shown in the main text.

2 The two-Higgs-doublet model

An extensive review of the 2HDM is available in reference [24], but this section will serve as an introduction to the model, its contributions to measurables, and its implementation in the context of this project.

2.1 Scalar doublet extensions of the Standard Model

Although the scalar sector of the SM has only been experimentally studied recently, leaving a more extensive scalar sector possible but unproven, there are certain constraints on what shape it may take. One particular limitation in $SU(2)\times U(1)$ gauge theory is the parameter ρ, which in general is given by [25]

$$\rho = \frac{\sum_i \left[I_i(I_i+1) - Y_i^2/4\right]|v_i|^2}{\sum_i Y_i^2 |v_i|^2/2} \tag{1}$$

at tree-level. Here I_i, Y_i, and v_i are the weak isospin, weak hypercharge, and vacuum expectation value (VEV) of all scalar multiplets Φ_i included in the theory respectively. The SM predicts ρ to be exactly 1 at tree-level, and current experimental measurements put it at $\rho = 1.00039 \pm 0.00019$ [20]. This puts stringent requirements on any theories which extend the scalar sector, but any multiplet with $I_i(I_i+1) = \frac{3}{4}Y_i^2$ will maintain $\rho = 1$, making $SU(2)$ singlets with $Y_i = 0$ and $SU(2)$ doublets with $Y_i = \pm 1$ prime candidates for scalar extensions [24].

Adding another scalar doublet, Φ_2, gives the potential (in the most general form) [24]:

$$
\begin{aligned}
V_{\text{2HDM}} = {} & m_{11}^2 \Phi_1^\dagger \Phi_1 + m_{22}^2 \Phi_2^\dagger \Phi_2 - \left(m_{12}^2 \Phi_1^\dagger \Phi_2 + \text{h. c.} \right) + \frac{\lambda_1}{2} \left(\Phi_1^\dagger \Phi_1 \right)^2 + \frac{\lambda_2}{2} \left(\Phi_2^\dagger \Phi_2 \right)^2 \\
& + \lambda_3 \left(\Phi_1^\dagger \Phi_1 \right) \left(\Phi_2^\dagger \Phi_2 \right) + \lambda_4 \left(\Phi_1^\dagger \Phi_2 \right) \left(\Phi_2^\dagger \Phi_1 \right) \\
& + \left[\frac{\lambda_5}{2} \left(\Phi_1^\dagger \Phi_2 \right)^2 + \lambda_6 \left(\Phi_1^\dagger \Phi_1 \right) \left(\Phi_1^\dagger \Phi_2 \right) + \lambda_7 \left(\Phi_2^\dagger \Phi_2 \right) \left(\Phi_1^\dagger \Phi_2 \right) + \text{h. c.} \right],
\end{aligned} \tag{2}
$$

where h. c. denotes Hermitian conjugates. The parameters m_{11}^2, m_{22}^2, and λ_i for $i \in \{1, 2, 3, 4\}$ must be real, but m_{12}^2 and λ_i for $i \in \{5, 6, 7\}$ may be complex [24]. This yields 14 degrees of freedom, although three are removed by the tadpole (one-legged 1-loop diagrams) equations (the condition that the potential is minimised), and another one can be removed by re-phasing one of the Higgs fields [26].

After a gauge transformation, the VEVs in this generic basis can be written as

$$
\langle \Phi_1 \rangle = \frac{1}{\sqrt{2}} \begin{pmatrix} 0 \\ v_1 \end{pmatrix} = \frac{v}{\sqrt{2}} \begin{pmatrix} 0 \\ c_\beta \end{pmatrix}, \qquad \langle \Phi_2 \rangle = \frac{1}{\sqrt{2}} \begin{pmatrix} 0 \\ v_2 e^{i\xi} \end{pmatrix} = \frac{v}{\sqrt{2}} \begin{pmatrix} 0 \\ s_\beta e^{i\xi} \end{pmatrix}, \tag{3}
$$

with v_1 and v_2 the VEVs of the respective scalar doublets and $v = \sqrt{v_1^2 + v_2^2}$, $c_\beta = \cos\beta$, $s_\beta = \sin\beta$, and $\tan\beta = \dfrac{v_2}{v_1}$. The W and Z boson masses squared, m_W^2 and m_Z^2, receive additive contributions from each v_i^2, meaning v here corresponds to the SM VEV [27], $v \approx 246$ GeV. Another convenient basis to work with, however, is the Higgs basis, in which only one doublet acquires a VEV [27]. A change of basis between the generic and Higgs bases can be performed by defining the unitary transformation matrix

$$
\hat{U} = \begin{pmatrix} \hat{v}_1^* & \hat{v}_2^* \\ \hat{w}_1^* & \hat{w}_2^* \end{pmatrix} = \begin{pmatrix} c_\beta & e^{-i\xi} s_\beta \\ -e^{i\xi} s_\beta & c_\beta \end{pmatrix}, \tag{4}
$$

where $\hat{v}_i$ are unit vectors in Higgs flavour space normalised such that $\hat{v}_a^* \hat{v}_a = 1$, and $\hat{w}_i \equiv -\epsilon_{ij} \hat{v}_j^*$ (with ϵ_{ij} being the Levi-Civita tensor) [28]. This gives the fields in the Higgs basis as $H_a = \hat{U}_{ab} \Phi_b$ (with inverse $\Phi_b = \hat{U}_{ba}^\dagger H_a$), giving the Higgs basis fields [26, 29]

$$
H_1 = \begin{pmatrix} G^\pm \\ \frac{1}{\sqrt{2}} \left(v + \varphi_1^0 + i G^0 \right) \end{pmatrix}, \qquad H_2 = \begin{pmatrix} H^\pm \\ \frac{1}{\sqrt{2}} \left(\varphi_2^0 + i a_0 \right) \end{pmatrix}. \tag{5}
$$

$G^\pm$ and G^0 are Goldstone bosons "eaten by $W^\pm$ and Z" after electroweak symmetry breaking, $H^\pm$ is a charged scalar field giving rise to charged scalar bosons, and $\varphi_{1,2}^0$ and a_0 mix together into three neutral Higgs particles, h_k^0. The scalar potential retains the form from the generic basis and will not be explicitly typeset, but can be found in references [26, 27, 29]. The Yukawa sector, however, will be presented in the Higgs basis, in which it reads (assuming massless neutrinos)

$$
\begin{aligned}
-\mathcal{L}_Y = {} & \overline{Q}_L \widetilde{H}_1 \kappa^U U_R + \overline{Q}_L H_1 \kappa^{D\dagger} D_R + \overline{L}_L H_1 \kappa^{L\dagger} E_R \\
& + \overline{Q}_L \widetilde{H}_2 \rho^U U_R + \overline{Q}_L H_2 \rho^{D\dagger} D_R + \overline{L}_L H_2 \rho^{L\dagger} E_R + \text{h. c.}\,.
\end{aligned}
\tag{6}
$$

Here, Q_L is the weak isospin quark doublet, L_L the weak isospin lepton doublet, and U_R, D_R, and E_R the corresponding weak isospin singlets. $\widetilde{H}_i \equiv i\sigma_2 H_i^*$, and κ^F and ρ^F are the Yukawa matrices in the Higgs basis. Particularly, the κ^F matrices are by construction diagonalisable with a biunitary transformation of the fermion fields [28], and are in fact the diagonal mass matrices [26]:

$$
\begin{aligned}
\kappa^U &= \frac{\sqrt{2}}{v}\,\mathrm{diag}(m_u, m_c, m_t), \\
\kappa^D &= \frac{\sqrt{2}}{v}\,\mathrm{diag}(m_d, m_s, m_b), \\
\kappa^L &= \frac{\sqrt{2}}{v}\,\mathrm{diag}(m_e, m_\mu, m_\tau).
\end{aligned}
\tag{7}
$$

The ρ^F matrices are not as simple to deal with. It is not typically possible to diagonalise both the κ^F and ρ^F matrices simultaneously, leaving the latter as arbitrary complex 3×3 matrices [28]. These potential off-diagonal elements leave flavour-changing neutral currents (FCNCs) possible, which will be discussed in more detail later. The ρ^F-matrices can be parametrised according to the Cheng-Sher ansatz [30]:

$$
\rho^F \equiv \lambda_{ij}^F \frac{\sqrt{2m_i m_j}}{v},
\tag{8}
$$

which allows for mass-supressed FCNCs when the λ_{ij}^F are of similar size. Reference [31] details upper limits on the off-diagonal elements $\lambda_{i\neq j}^F$ in the quark sector based on neutral meson oscillations, and reference [32] gives similar restrictions for the lepton sector. These are all of the order $|\lambda_{i\neq j}^F| \lesssim 10^{-1}$.

2.2 Theoretical limitations

There are several theoretical constraints on any scalar extension in BSM theories. Three of the most important ones are perturbativity, unitarity, and stability, which will be detailed here.

Perturbativity refers to the potential breakdown of perturbation theory in the quartic couplings of the scalar fields. The magnitudes of the generic basis parameters λ_i may not grow too large upon renormalisation, typically imposed as an upper limit $|\lambda_i| < 4\pi$ for every individual λ_i [33]. For quartic scalar couplings, perturbation theory may actually break down at smaller coupling values than this, but they will definitely run fast for $|\lambda_i| > 4\pi$,

making this limit an approximation for the scale where a Landau pole is encountered [33, 34].

The unitarity condition refers to unitarity of the Higgs-Higgs scattering matrices, which at high enough energies contain only s-wave amplitudes at tree level [35]. These tree-level scattering matrices $\Lambda_{Y\sigma}$ (with Y total hypercharge and σ weak isospin) are worked out in reference [35], and hold exclusively elements λ_i. The unitarity constraint forces the eigenvalues of these matrices $|\Lambda_{Y\sigma}|$ to be less than $(8\pi)^{-1}$, putting additional limitations on the λ_i parameters. Note that the scattering matrices in reference [35] only apply for large scattering energies $\sqrt{s}$, and that more careful attention may have to be taken at lower energies to further constrain the parameter space [36], although these restrictions are not applied in this project.

Tree-level scalar potential stability, or stability for short, is the condition that the scalar potential is bounded from below, i.e. that it has a global minimum. References [37, 38] develop a Minkowskian formalism of the general 2HDM. In this formalism, the scalar potential can be written with a tensor $\Lambda^{\mu\nu}$ constructed using the λ_i parameters, with the requirement that "the tensor $\Lambda^{\mu\nu}$ is positive definite on the future light-cone" [37]. This is equivalent with $\Lambda^{\mu\nu}$ being diagonalisable by an $SO(1,3)$ transformation, with four linearly independent eigenvectors associated with four eigenvalues, the largest of which must be timelike and larger than zero. Reference [39] shows that parameter regions ruled out by tree-level stability conditions may be saved by 1-loop corrections, but these corrections are excluded in this project.

2.3 Magnetic and electric dipole moments of leptons

The spin magnetic moment $\boldsymbol{\mu}$ of charged spin-$\frac{1}{2}$ point particle is given by $\boldsymbol{\mu} = \frac{ge}{2m}\mathbf{S}$, where e is the electron charge, m is the particle mass, $\mathbf{S}$ is the spin angular momentum, and g is the so-called g-factor [40]. At tree-level, g is predicted to be identically 2 for all such particles, but higher order corrections from loops predicts a slight deviation, called the anomalous magnetic dipole moment (AMM) $a = \frac{1}{2}(g-2)$. The SM prediction for the electron AMM is approximately $a_e \approx 1.16 \times 10^{-3}$, differing from current experimental results by 1 in 10^{12}, or about 2 σ [41].

The muon AMM, a_μ, is not as well-known. The difference between experimental measurements and the SM prediction, $\Delta a_\mu = a_\mu^{\text{exp}} - a_\mu^{\text{th}}$, is $268(76) \times 10^{-11}$ [20], a difference of 3.5 σ. This deviation is not sizable enough to say anything definitive, but until more precise experimental and theoretical results are obtained it can be used as one way to characterise BSM models, as new Feynman diagrams resulting from any BSM extensions may contribute to a_μ, and could thus explain Δa_μ (should it survive future experiments). In the case of the 2HDM, some of these contributions have been studied in reference [42], among others.

Due to how spin transforms under parity and time reflection, a non-zero electric dipole moment (EDM) of a fundamental particle would indicate some sort of $\mathcal{CP}$-violation [43], and although the $\mathcal{CP}$-violating terms in the SM do predict a non-zero electron EDM $|d_e| \lesssim 8.6 \times 10^{-38}\ e$ cm [44], this is several orders of magnitude smaller than the current upper

experimental bound of $1.1 \times 10^{-29}\, e$ cm [23]. The 2HDM contributions to d_e have been studied extensively [45–48], and can generally be of orders of 10^{-30} to 10^{-26} [49]. Thus possible 2HDMs can be ruled out by analysis of their d_e contributions.

2.4 Hard and soft $\mathbb{Z}_2$-violation

One possible issue with the 2HDM is the existence of tree-level flavour-changing neutral currents (FCNCs), interactions in which fermions change flavour without changing electric charge. These are a direct result of the inability to diagonalise the ρ^F-matrices in eq. 6, as off-diagonal elements imply flavour-changing Feynman diagram vertices. Experimental limits on any such interactions are stringent [20], making the suppression of them a key aspect of BSM models. In the 2HDM, FCNCs can be avoided through alignment of the flavour space-representations Yukawa matrices [50], i.e. restricting the model to the case when the κ^F- and ρ^F-matrices are simultaneously diagonalisable and mutually proportional, $\rho^F = a^F \kappa^F$ for some alignment parameter $a^F \in \mathbb{C}$.

Another, more robust, way to achieve this is to impose a so-called $\mathbb{Z}_2$ symmetry. The set of nth roots of unity, $\mathbb{Z}_n$, is a group under multiplication. A $\mathbb{Z}_2$ symmetry is then a discrete multiplicative two-charge symmetry, with even $(+1)$ and odd (-1) charges. By restricting the model to the case when the Higgs doublets have opposite charges and each right handed fermion doublet has a specific charge, the model reduces to exactly four different types of aligned 2HDMs (A2HDMs) [51], as shown in Table 1. Fixing the generic potential in eq. 2 to the $\mathbb{Z}_2$ symmetry obviously requires $m_{12}^2 = \lambda_6 = \lambda_7 = 0$, and the basis-dependent parameter $\tan\beta$ attains physical significance as a proper parameter.

Table 1: The four $\mathbb{Z}_2$-symmetric 2HDM types. Φ_1 is odd (-1) and Φ_2 is even $(+1)$, and the Yukawa matrices are aligned such that $\rho^F = a^F \kappa^F$.

Type	U_R	D_R	L_R	a^U	a^D	a^L
I	$+$	$+$	$+$	$\cot\beta$	$\cot\beta$	$\cot\beta$
II	$+$	$-$	$-$	$\cot\beta$	$-\tan\beta$	$-\tan\beta$
X	$+$	$+$	$-$	$\cot\beta$	$\cot\beta$	$-\tan\beta$
Y	$+$	$-$	$+$	$\cot\beta$	$-\tan\beta$	$\cot\beta$

A 2HDM with an exact $\mathbb{Z}_2$ symmetry is $\mathcal{CP}$-conserving, as the only remaining complex parameter, λ_5, can be made real with a rephasing transformation [26, 51]. It is possible to add a so-called soft $\mathbb{Z}_2$-violation by dropping the restriction that $m_{12}^2 = 0$, but retaining the conditions $\lambda_6 = \lambda_7 = 0$. Although this allows for mixing between the Φ_1 and Φ_2 fields, the $\mathbb{Z}_2$ symmetry is respected at small distances for all orders of perturbation, meaning any $\Phi_1 \longleftrightarrow \Phi_2$ transitions disappear as virtuality $q^2 \to \infty$ [51]. This soft $\mathbb{Z}_2$-violation allows $\mathcal{CP}$-violation to enter the model while maintaining the benefits of the $\mathbb{Z}_2$ symmetry. The general 2HDM potential, with quartic couplings λ_6 and λ_7 not identically zero, is considered the hard $\mathbb{Z}_2$-violating case, as it has the $\mathbb{Z}_2$ symmetry broken at large and small distances alike [51].

2HDMs with softly broken $\mathbb{Z}_2$ symmetries have been studied extensively [24], particularly the Type II models, as they correspond to the scalar sector of minimal supersymmetric SM extensions [52] (which need up- and down-type quarks to couple to different scalar fields). Certain parameter space regions of these "softly $\mathbb{Z}_2$-symmetric" models have been shown to not be excluded by experimental data, but do not contribute remarkably to Δa_μ [53]. Hence, if Δa_μ is not eradicated with future experimental data, a softly $\mathbb{Z}_2$-symmetric 2HDMs would also necessitate some additional new physics to explain this discrepancy. For this reason, no "proper" $\mathbb{Z}_2$ symmetry is assumed for the purposes of this project.

2.5 The Two-Higgs-Doublet Model Evolver

The Two-Higgs-Doublet Model Evolver (`2HDME`) is a `C++11` API by Oredsson [34, 54], developed for studying renormalisation group equation (RGE) evolution of the general 2HDM. Although the primary scope of `2HDME` is to solve the RGEs, it also has functionality for treating 2HDMs in general. The `EDM` class is an object which can be used to calculate d_e contributions from a given 2HDM, and will be used for this exact purpose. For a full description of `2HDME`, the manual is available in reference [34].

`2HDME` has its main utility in the `THDM` class, which is an object representing a general 2HDM. It must be initialised with a SM, in the form of a `SM` object, which sets gauge couplings and the VEV, defined at the m_Z scale. To define the 2HDM, the generic (although other bases are defined as well) scalar potential parameters λ_i and $|m_{12}^2|$, and $\tan\beta$, need to be set (m_{11}^2, m_{22}^2, the phase of m_{12}^2, and the VEV phase ξ are all set by the tadpole equations), as well as the Yukawa sector. The Yukawa sector can be defined using one of the four $\mathbb{Z}_2$-symmetric types detailed in Section 2.4, three alignment parameters a^F for an A2HDM, or three general complex 3×3 ρ^F-matrices.

`EDM` class objects are initialised using a `THDM` type object, and calculate the 2HDM contributions to d_e using the Barr-Zee 2-loop diagrams (described in Section 3.2), with the couplings in each individual loop defined at the energy scale of the heaviest participating particle (with the `THDM` object evolved using the API's own renormalisation group functionality). The program can then return a vector containing all the individual contributions, as well as a sum of these as the total d_e contribution.

However, `2HDME` does not include 1-loop contributions to d_e (although these are typically dominated by the Barr-Zee diagrams [42]), nor can it calculate a_μ contributions. For this project, the program needs to be extended to treat these. While the 1-loop integral must be done from scratch, Oredsson and Rathsman [49] remark that the Barr-Zee a_μ contributions are effectively the same as the d_e contributions, except with the real parts of the Yukawa couplings instead of the imaginary, making modifications to account for 2-loop a_μ contributions simple.

3 Practical and analytic developments

3.1 Flavour-mixing 1-loop diagrams

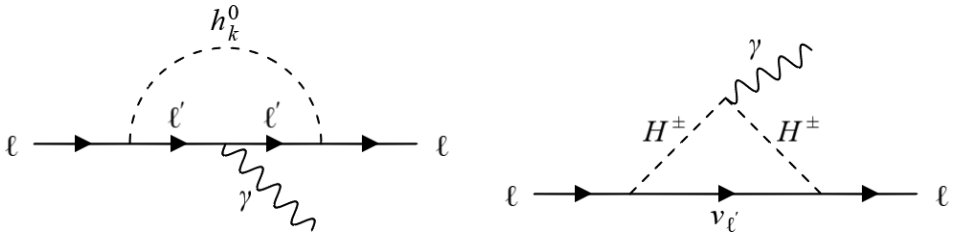

(a) Neutral boson loop. **(b)** Charged boson loop.

Figure 1: 1-loop Feynman diagrams contributing to lepton AMMs and EDMs for a general 2HDM with FCNCs.

Although the 1-loop Feynman diagrams arising in 2HDMs have been analysed previously, descriptions have typically been limited to aligned-type models [42, 53]. Any non-zero off-diagonal elements in the leptonic part of the Yukawa sector, i.e. a non-diagonalisable ρ^L, will give rise to first order loops of the form shown in Figure 1, with $\ell \neq \ell'$. The A2HDM loops, corresponding to the Yukawa matrix diagonals, correspond to $\ell = \ell'$, so a general implementation of the 1-loop also includes these. A short note on how these generic analytic expression were acquired is available in Appendix A.

The generalised d_ℓ and a_ℓ neutral Higgs 1-loop contributions are found to be

$$a_\ell^{\text{1-loop}} = \frac{m_\ell}{8\pi^2} \sum_{\ell',k=1}^{n} \int_0^1 dx \int_0^x dy \frac{(y-1)\left(y\,\text{Re}\left(\left(Y_{\ell\ell'}^{h_k^0}\right)^* Y_{\ell'\ell}^{h_k^0}\right) m_\ell + \text{Re}\left(Y_{\ell\ell'}^{h_k^0} Y_{\ell'\ell}^{h_k^0}\right) m_{\ell'}\right)}{m_\ell^2\left[y(y-x)+(1-y)\right] + m_{h_k^0}^2 y}, \quad (9)$$

$$d_\ell^{\text{1-loop}} = \frac{e}{16\pi^2} \sum_{\ell',k=1}^{n} \int_0^1 dx \int_0^x dy \frac{(y-1)\left(y\,\text{Im}\left(\left(Y_{\ell\ell'}^{h_k^0}\right)^* Y_{\ell'\ell}^{h_k^0}\right) m_\ell + \text{Im}\left(Y_{\ell\ell'}^{h_k^0} Y_{\ell'\ell}^{h_k^0}\right) m_{\ell'}\right)}{m_\ell^2\left[y(y-x)+(1-y)\right] + m_{h_k^0}^2 y}. \quad (10)$$

Here, $Y_{\ell\ell'}^{h_k^0}$ is the scalar boson h_k^0's coupling for the transition $\ell \to \ell'$, m_i is the mass of a particle i, the sum ℓ' is over all accessible neutral flavour changing vertices, and the sum k is over the neutral scalar bosons that can mediate the interaction. The lepton mass terms m_ℓ^2 in the denominators are four-momentum terms, which do not depend on $m_{\ell'}$, meaning any $m_{\ell'}$ terms are exclusively in the numerators. The charged Higgs vertices are excluded, based on the assumption that neutrinos do not couple to either Higgs doublet.

Should the EDMs and AMMs for quarks be desired, these integrals could be reapplied to the quark sector by exchanging each lepton index with a correspond quark index, although

the charged Higgs vertices would then instead be a quark-type exchange between the up- and down-families.

3.2 Barr-Zee 2-loop diagrams

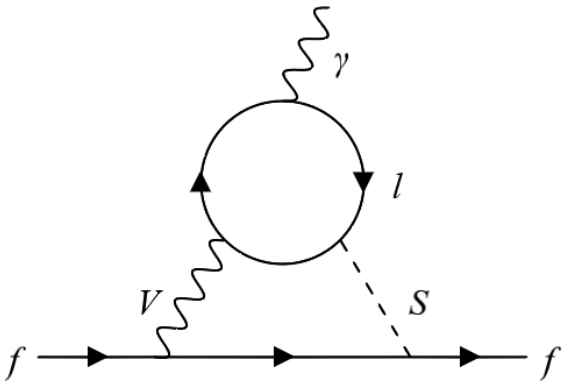

Figure 2: The general structure of Barr-Zee two-loop diagrams, where V is a vector boson and S is a scalar boson, and the loop particle l in general is any massive fermion or boson.

The 2-loop Barr-Zee digrams [55], illustrated in Figure 2 and first calculated for 2HDM in reference [56], generate the dominant contributions to the EDMs [57] and AMMs [42] of light fermions in 2HDMs. They are characterised by the couplings of one vector boson V, one scalar boson S, and one loop particle l (making up the central loop in the figure). Just as for the 1-loop, these have typically been studied in the context of soft $\mathbb{Z}_2$-violation, but analytic expressions for d_e contributions in the general 2HDM are available in reference [49], and as `C++` code in `2HDME` [34]. The AMM contributions can be calculated with similar expressions to those in [49], but with the real parts of the Yukawa couplings rather than the imaginary. For this project, the extant implementation of Barr-Zee d_e contribution calculations in the `2HDME` API could be repurposed to calculate the Barr-Zee a_μ contributions with only minor modifications, by comparison with reference [42].

3.3 Modifications to 2HDME

3.3.1 1-loop integrals

As mentioned in Section 2.5, `2HDME` does not have tools for calculating any 1-loop diagram contributions, nor does it calculate the Barr-Zee diagram contributions to a_μ, necessitating modifications for the purposes of this project. Details on how to extend `2HDME` with these additions are available in Appendix B.

Numerical implementation of eqs. 9 and 10 were done using the two-dimensional trapezoidal rule by defining the inner integral argument as functions $f(x, y)$ and performing the

trapezoidal approximation of the two integrals sequentially, resulting in the general expression for the integral

$$\int_0^1 dx \int_0^x f(x,y)dy \approx$$
$$\frac{1}{m}\left[\frac{f(0,0)}{2} + \frac{f(0,0)+f(1,1)}{n} + \frac{1}{n}\left\{\sum_{j=1}^{n}\left(f\left(\frac{j}{n},\frac{j}{n}\right) + \sum_{i=1}^{m} f\left(\frac{j}{n},\frac{ij}{mn}\right)\right)\right\}\right]. \tag{11}$$

The programmed implementation is slightly more involved, using an adaptive upper limit for the inner sum so as to maintain consistent resolution for each step of the outer sum, but this is a simple condition that $m = kj$ for some positive integer $k \in \mathbb{Z}^+$.

As `2HDME` has built-in functionality for calculating the Barr-Zee d_e contributions, much of the original code could be repurposed for a_μ contribution calculation. Comparisons with reference [42] were made to verify the analytic expressions. All inherent functionality for the d_e contributions was remade to support the a_μ contributions. Besides the ability to calculate individual diagram and total contributions, this also includes the ability to print contributions to the console, or to save them as `SLHA` blocks that can be saved to datafiles using `2HDME` itself.

3.3.2 Software discussion

For the purposes of this project, four different tools were developed to help with the analysis of 2HDMs: A modified `EDM` class (based on the one included in the `2HDME` API), to support a_μ contribution calculation; as well as three programs, called `2hdmSearcher`, `phaseTester`, and `magTester`. The discussion here will be focused on their purpose and what extensions could be made to increase their applicability. Instruction manuals on where to acquire them and how to apply them practically are available in Appendix B.

The main development, and the core of the three programs used in the parameter study performed for this project, is the a_μ calculation extension of the `2HDME` API, making the possible analysis of 2HDMs using `2HDME` more extensive than previously. With the a_μ calculation implemented, modification for calculation of the AMM contributions to other fermions would also be simple, which could allow for more extensive restrictions on analysed 2HDMs by e.g. checking that electron AMM contributions would not become too large.

`2hdmSearcher` is a tool made for the purpose of randomly searching for 2HDMs based on maximal $|d_e|$ and a minimum a_μ contributions. It is built to initialise the ρ^F-matrices with all diagonal λ_{ii}^F factors (under the Cheng-Sher ansatz) equal for each individual fermion-type F, but the off-diagonal elements are allowed to run free. Although this project has strictly used real ρ^F-matrices, `2hdmSearcher` does allow for a complex Yukawa sector by adding a random phase to the ρ^F-matrix elements. This program could potentially be used for generating a large amount of random 2HDMs in order to collect aggregate data for larger parts of the parameter space, although further checks may be needed to the program based on desired properties of parameter points.

The two programs used for analysis are `phaseTester` and `magTester`. The former takes an input 2HDM with a softly $\mathbb{Z}_2$-violating potential and an arbitrary real ρ^L-matrix and varies the phase of λ_5 around the unit circle, to show how $|d_e|$ and a_μ contributions vary with the amount of $\mathcal{CP}$-violation allowed in the potential. `magTester`, on the other hand, calculates the $|d_e|$ and a_μ contributions for an arbitrary 2HDM potential as functions of the magnitude of the ρ^L-matrix, by multiplying either the entirety or only the diagonal of an arbitrary input real ρ^L-matrix with a real magnification factor M, over a user-input interval. Both programs assume that ρ^U and ρ^D are aligned, with $a^U = a^D = 1$, but could easily be extended to take user input parameters for these matrices as well.

4 Parameter study

This section details the parameter spaces which have been scanned, as split into three different regions depending on scalar potentials and Yukawa sectors. Some point studies are made for each of these regions to detail how they develop with Yukawa sector magnitude (in the form of enhanced Higgs basis ρ^L-matrices) to show how they could or could not simultaneously explain Δa_μ while giving a $|d_e|$ within experimental bounds. Note that no $\mathbb{Z}_2$ symmetry is applied to the Yukawa sector.

Although the lepton part of the Yukawa sector will be varied for these parameter scans, the quark sector is assumed to be aligned with alignment factor 1, i.e. $\kappa^U = \rho^U$ and $\kappa^D = \rho^D$. Ilisie [42] shows that variation in the quark alignment factors will have little effect on a_μ, and although untested this should also apply to d_e contributions (assuming a real alignment factor). The Yukawa sector will also be assumed to be entirely real. As in [49], the scalar potential will be restricted to the region:

$$|\lambda_i| \leq 2, \qquad |\lambda_j| \leq 0.5, \qquad |m_{12}^2| \in [10^2, 2\times 10^5], \qquad \tan\beta \in [1, 50], \tag{12}$$

for $i \in \{1,2,3,4,5\}$ and $j \in \{6,7\}$. The phase of m_{12}^2 is fixed from the tadpole equations, and any other phases randomly generated.

Under these assumptions, three different parameter regions are studied:

Region I: Softly $\mathbb{Z}_2$-violating potential with aligned Yukawa sector.

This parameter region is defined with the potential parameter region as in eq. 12, with the restriction $\lambda_6 = \lambda_7 = 0$, and all ρ^F-matrices diagonalisable and proportional to the diagonal mass-matrices. Although similar to the $\mathbb{Z}_2$-symmetric models, the independence of parameters in the Yukawa sector in these models could provide regions of interest not found in the $\mathbb{Z}_2$-symmetric ones.

Region II: Softly $\mathbb{Z}_2$-violating potential with undiagonalisable Yukawa sector.

For this region, the scalar potential is set identically as in region I, but the ρ^F-matrices — particularly, the ρ^L-matrix — are allowed to be more general (albeit still real) matrices.

Using the Cheng-Sher parametrisation (eq. 8), two particular cases are studied and compared: An enhanced semi-aligned ρ^L-matrix, in which ρ^L is first defined with the diagonal elements $\lambda^L_{ii} = 1$, and $\lambda^L_{ij} \in [10^{-2}, 10^{-1}]$ for $i \neq j$, and the entire matrix is then enhanced by a real magnification factor $M \in [1, 50]$, equivalent with a redefinition of $\lambda^L_{ij} \to M\lambda^L_{ij}$; and a diagonally enhanced semi-aligned ρ^L-matrix, in which ρ^L is initialised as in the regular enhanced case for $M = 1$, but the enhancement is applied only to the diagonal, a redefinition $\lambda^L_{ii} \to M\lambda^L_{ii}$ and $\lambda^L_{ij} \to \lambda^L_{ij}$ for $i \neq j$. As mentioned in Section 2.1, experimental bounds on FCNCs puts restrictions on off-diagonal elements at $|\lambda^L_{i\neq j}| \lesssim 10^{-1}$, meaning the fully enhanced case is viable only for small magnification factors, $M \leq 10$. For larger values of M it does still provide a comparison for the diagonally enhanced case, however, but should not be viewed as proper candidates for parameter spaces.

Region III: Hard $\mathbb{Z}_2$ violation with undiagonalisable Yukawa sector.

This is an almost fully generalised region. The restrictions on $\lambda_{6,7}$ are dropped, and the Yukawa sector is parametrised identically to region II, with focus on an enhanced semi-aligned and an enhanced diagonal semi-aligned lepton sector.

Certain restrictions are made as to what parameter points are studied. Any 2HDM for which the lightest neutral scalar boson is dissimilar to the SM one and the one discovered in 2012 is discarded (enforced with mass comparison, requiring the lightest neutral boson to be in the range $m_{h_1} \in [120, 130]$ GeV). Said 2HDM must then survive RGE evolution up to the mass of the heaviest scalar boson, should it be larger than the top quark mass, and must also fulfill the theoretical conditions detailed in Section 2.2. Moreover, parameter points which give a sizeable Δa_μ (of order 10^{-9}) while giving rise to an experimentally bounded electron EDM, $|d_e| \leq 10^{-29}$, are studied extensively. Due to the rare nature of such points (only some hundred having been found after searching tens of millions of parameter points), no aggregate data study of these will be performed. Instead, point studies will be provided to prove their existence and to showcase the nature such candidates may have.

4.1 Region I

A real aligned Yukawa sector, or any model with simultaneously diagonalisable real κ^F- and ρ^F-matrices in general, will not generate any 1-loop d_e contributions at the electroweak scale. Any analysis of them will be left to regions II and III. However, 1-loop a_μ contributions do exist. They can for larger alignment factors become sizeable, and will thus be studied.

Two parameter points, $\mathbf{P_1}$ and $\mathbf{P_2}$ (as defined in Table 2) are analysed (with figures depicting analysis of $\mathbf{P_2}$ available in Appendix C), where $\mathbf{P_1}$ was able to generate a sizeable $\Delta a_\mu \approx 2 \times 10^{-9}$ while generating a $|d_e| \approx 10^{-30}$ e cm, while $\mathbf{P_2}$ is an arbitrary point that was discarded during the search for points like $\mathbf{P_1}$, due to providing too large a total contribution to $|d_e|$. The effects of variation of $\arg(\lambda_5)$ and alignment factor a^L are henceforth detailed.

Figure 3 depicts the variation of $\mathbf{P_1}$ scalar boson masses with $\arg(\lambda_5)$. For $\arg(\lambda_5) \approx \pi$,

Table 2: The two parameter points studied for region I. The phase of λ_5 and the alignment factor a^L are allowed to vary freely, while $a^U = a^D = 1$.

	$\mathbf{P_1}$	$\mathbf{P_2}$
$\tan\beta$	1.3440	7.422
$\lvert m_{12}^2\rvert$	64586.3	78834.5
λ_1	0.86236	1.8870
λ_2	0.98722	0.18113
λ_3	1.2431	0.90683
λ_4	−1.1061	1.4829
$\lvert\lambda_5\rvert$	0.64660	1.2448

$\mathbf{P_1}$ gives a lightest neutral mostly $\mathcal{CP}$-even (the $\mathcal{CP}$-odd component of the eigenvector being of order 10^{-2}) Higgs boson at 126.7 GeV, making it similar to the one discovered in 2012. In Figures 4 and 5, the dependence of $|d_e|$ and a_μ on a^L and $\arg(\lambda_5)$ are detailed. The former shows cancellation among individual d_e contributions for all phase values, resulting in parameter regions where a_μ contributions can be of the order of Δa_μ, as seen in Figure 5, while total 2-loop d_e contributions are orders of magnitude smaller than experimental bounds without explicitly requiring a mostly real λ_5. As only the absolute value of the total d_e contribution has been studied, it is possible that the black curve in Figure 4 correspond to a sign change for d_e contributions.

Unlike $|d_e|$, a_μ is largely unaffected by the phase variation: Its maximum changes in magnitude by a third, and Figure 6 shows that the 1-loop contribution also differs very little with $\arg(\lambda_5)$. Although largely insignificant at small a^L, Figure 6 also shows that the 1-loop contribution can account for upwards of 10% of total a_μ contributions for large magnitudes of a^L. Overall, however, total a_μ contributions reach the same order as Δa_μ for large magnitudes of the Yukawa lepton couplings, $30 \leq a^L$.

4.2 Region II

For this region, ρ^L is initialised with the Cheng-Sher ansatz such that $\lambda_{ii}^L = 1$, and off-diagonal elements $\lambda_{ij} \in [10^{-2}, 10^{-1}]$ for $i \neq j$. This results in tree-level FCNCs at the electroweak scale, and gives rise to 1-loop d_e contributions. One particular 2HDM called $\mathbf{P_3}$, detailed in Table 3, will be considered, as well as an undiagonalisable extension of $\mathbf{P_1}$ described in Table 2, called $\mathbf{P_1^*}$, which is also described in Table 3.

In this section, $\mathbf{P_3}$ will be analysed in detail, whereas for $\mathbf{P_1^*}$ magnitude analysis is shown in Figure C.4. A phase portrait of $\mathbf{P_3}$ is available in Figure 7. Studies into the magnitude effects on d_e and a_μ are made at two values of $\arg(\lambda_5)$: The $|d_e|$ maximum at $\arg(\lambda_5) = 0.613$, and close to the second zero, $\arg(\lambda_5) = \pi - 10^{-3}$. At the latter phase, the mass of the lightest Higgs boson is 126.26 GeV, and it is almost exclusively made up of $\mathcal{CP}$-even constituents (with $\mathcal{CP}$-odd component of the eigenvector being of order 10^{-4}),

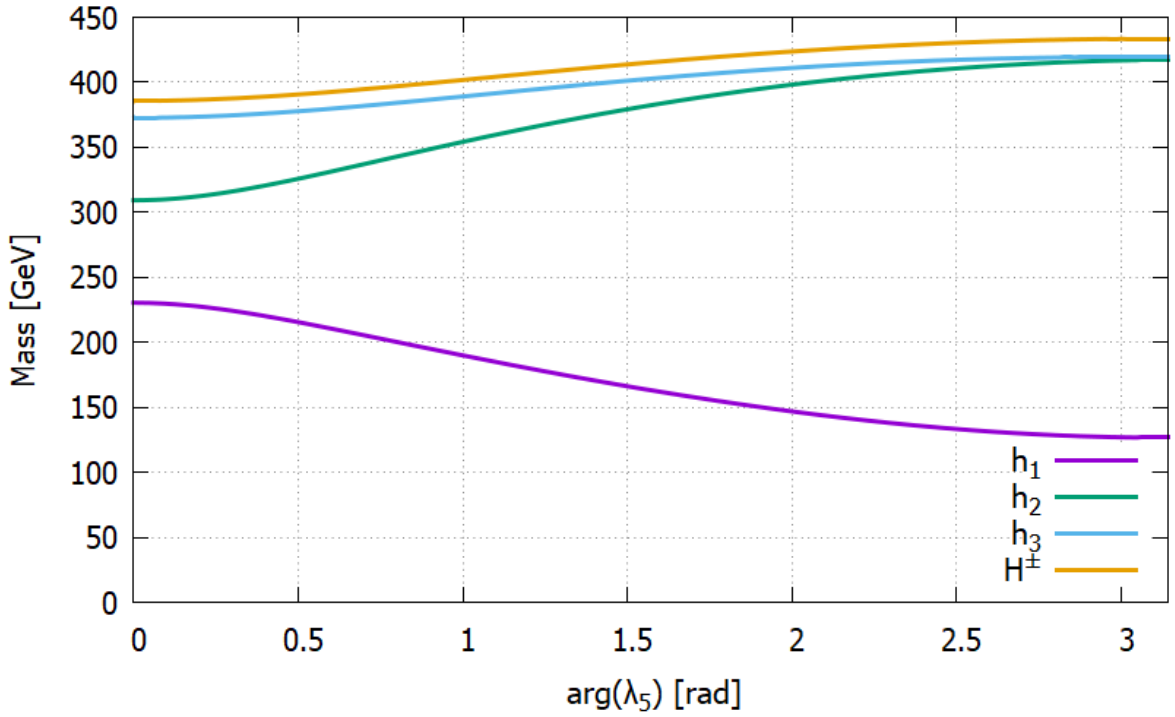

Figure 3: Variation of scalar boson masses with $\arg(\lambda_5)$ for the 2HDM defined at $\mathbf{P_1}$ in Table 2 h_i denotes a neutral boson, while $H^{\pm}$ denotes a charged boson.

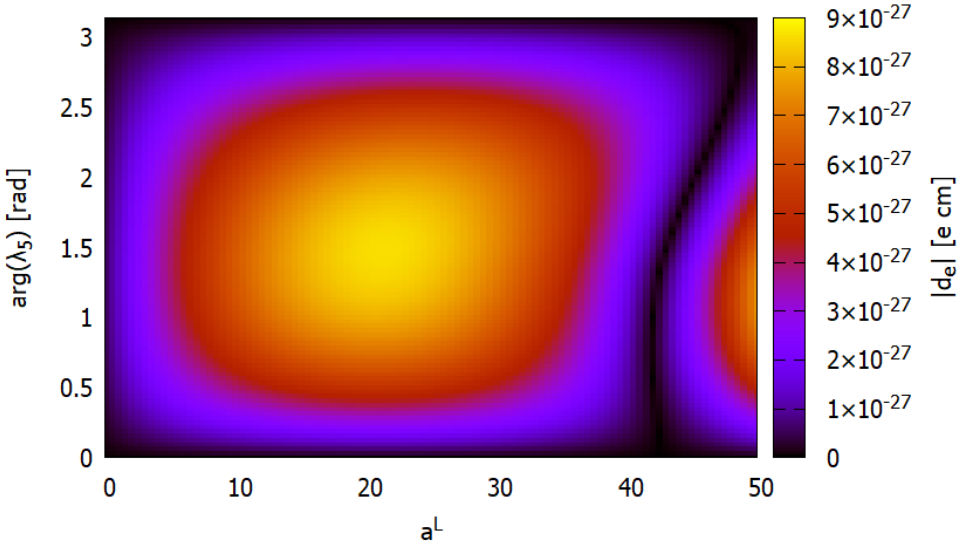

Figure 4: Variation of $|d_e|$ with a^L and $\arg(\lambda_5)$ at $\mathbf{P_1}$, as defined in Table 2. The dip in $|d_e|$ for $\arg(\lambda_5) \approx \pi$ at $a^L = 47.25$ (more clearly visible in figure C.3, due to the difference in orders of magnitude) gives a lightest neutral Higgs boson mass of 126.7 GeV and $\Delta a_\mu = 1.95 \times 10^{-9}$.

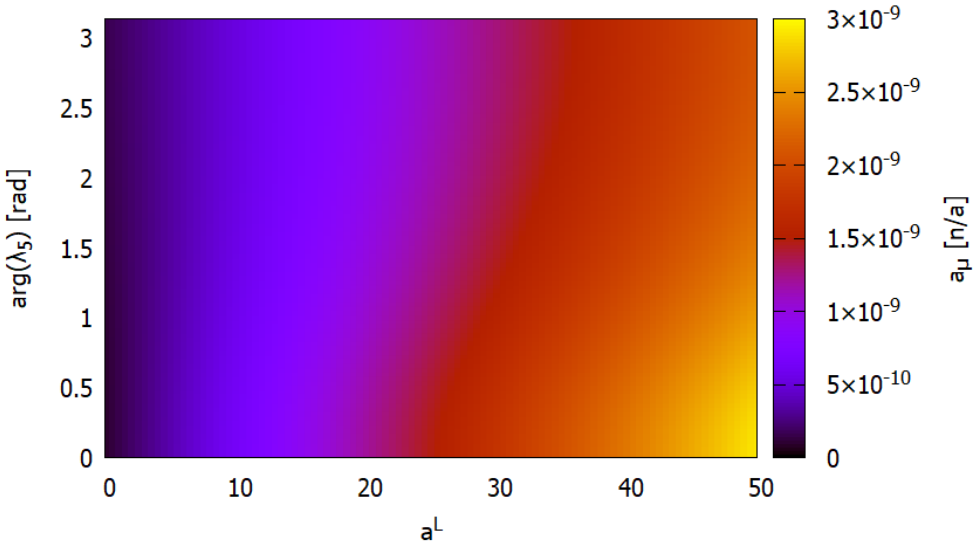

Figure 5: Variation of a_μ contributions with a^L and $\arg(\lambda_5)$ at $\mathbf{P_1}$ as in Table 2. Variation of $\arg(\lambda_5)$ results in a slight shift of the a_μ contribution at a given a^L.

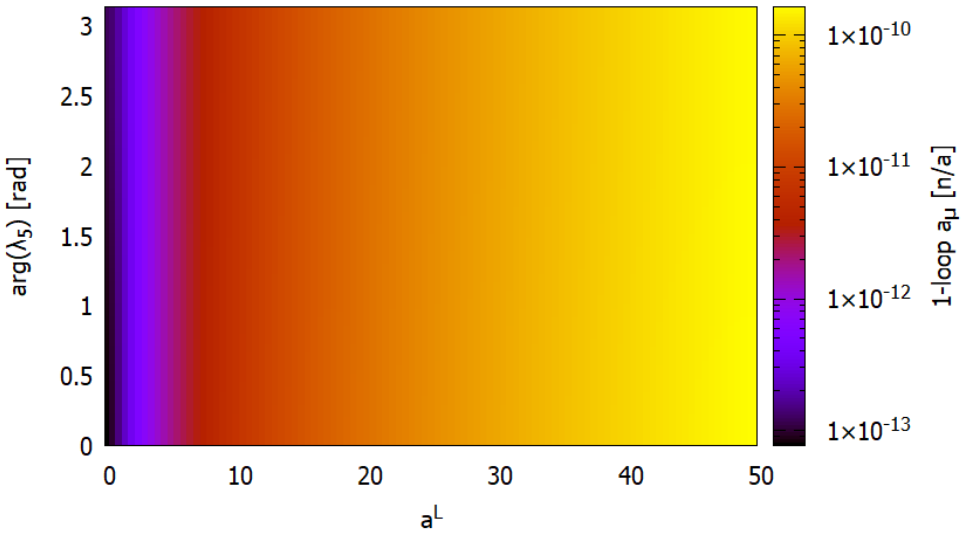

Figure 6: The 1-loop contribution to a_μ for the 2HDM defined at $\mathbf{P_1}$ in Table 2 as functions of $\arg(\lambda_5)$ and a^L. Although insignificant at small a^L, the 1-loop contribution to a_μ constitutes upwards of 10% of the total contribution for large a^L.

Table 3: The two parameter points studied for region II. The phase of λ_5 and the magnification factor M of the ρ^L matrix are allowed to run free, while the quark sector is aligned with $a^U = a^D = 1$. The diagonal λ_{ii} elements are equal to 1.

	$\mathbf{P_1^*}$	$\mathbf{P_3}$
$\tan\beta$	1.3440	1.94809
$\lvert m_{12}^2\rvert$	64586.3	20728.3
λ_1	0.86236	0.38645
λ_2	0.98722	0.3466
λ_3	1.2431	1.79558
λ_4	−1.1061	−1.1219
$\lvert\lambda_5\rvert$	0.64660	0.57216
$\lambda_{e\mu}^L$	0.1	0.03303
$\lambda_{e\tau}^L$	0.1	0.07375
$\lambda_{\mu e}^L$	0.1	0.01427
$\lambda_{\mu\tau}^L$	0.1	0.04320
$\lambda_{\tau e}^L$	0.1	0.01668
$\lambda_{\tau\mu}^L$	0.1	0.08134

making it similar to the scalar boson discovered in 2012. Figure 7a shows a maximum for a_μ as a function of the potential phase at $\arg(\lambda_5) \approx 1$, meaning a_μ is not a strictly increasing or decreasing function of $\arg(\lambda_5)$ in the interval $[0, \pi]$.

The effects of enhancing the entirety of and the diagonal of ρ^L for $\mathbf{P_3}$ are displayed in Figure 8. In Figure 8b, the fully and diagonally enhanced values for $|d_e|$ are indistinguishable at the resolution of the figure. For the minimal $|d_e|$ phase shown in Figure 8a, the variation is comparatively larger, being a factor 10^{-2} smaller than the magnitudes. Compare this to Figure C.4 depicting $\mathbf{P_1^*}$, where the position of the $|d_e|$ minimum is visibly offset along the M-axis for the different enhancement cases. Notable here is how variation of $\arg(\lambda_5)$ seems to put a possible $|d_e|$ contribution zero point (or sign change) far outside the studied magnitude region, as Figure 8b shows total $|d_e|$ contributions growing almost linearly with with M for $\mathbf{P_3}$ at $\arg(\lambda_5) = 0.613$.

The 1-loop contributions to a_μ and $|d_e|$ can be seen in Figure 9. The a_μ contribution follows a similar evolution for all four cases, although the fully enhanced and diagonally enhanced cases differ by a factor 2 consistently for sufficiently large values of the magnification factor M. 1-loop contributions to $|d_e|$ show more variation in behaviour: The fully enhanced cases are similar in form, but the diagonally enhanced case shows close to no dependence on M for $\mathbf{P_3}$ at $\arg(\lambda_5) = 0.613$, but in the $\arg(\lambda_5) \approx \pi$ case it decreases with increasing M. Whether this is a case of cancellation from different loops or a decrease in magnitude of individual loops has not been studied.

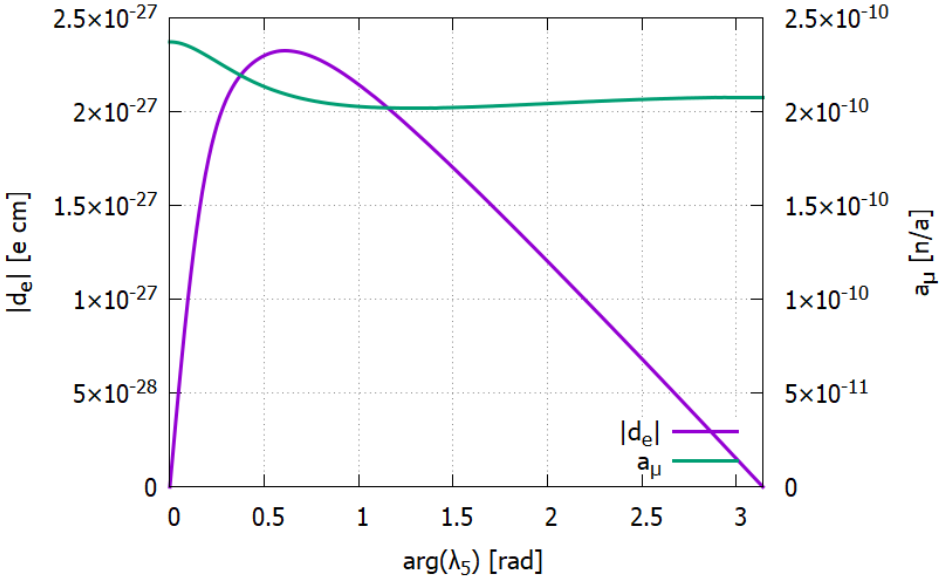

(a) $|d_e|$ and a_μ variation.

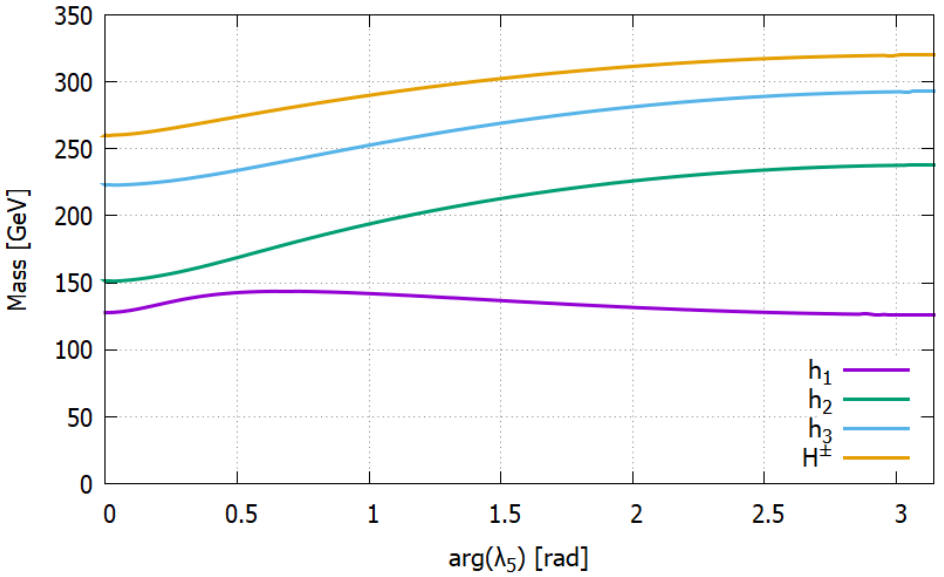

(b) Scalar boson mass variation. h_i denotes a charge neutral boson, while $H^\pm$ denotes a charged boson.

Figure 7: Variation of $|d_e|$ and a_μ (7a) and scalar boson masses (7b) with $\arg(\lambda_5)$ for the 2HDM defined at $\mathbf{P_3}$ in Table 3 with diagonal elements of ρ^L defined with the Cheng-Sher ansatz as $\lambda_{ii} = 1$.

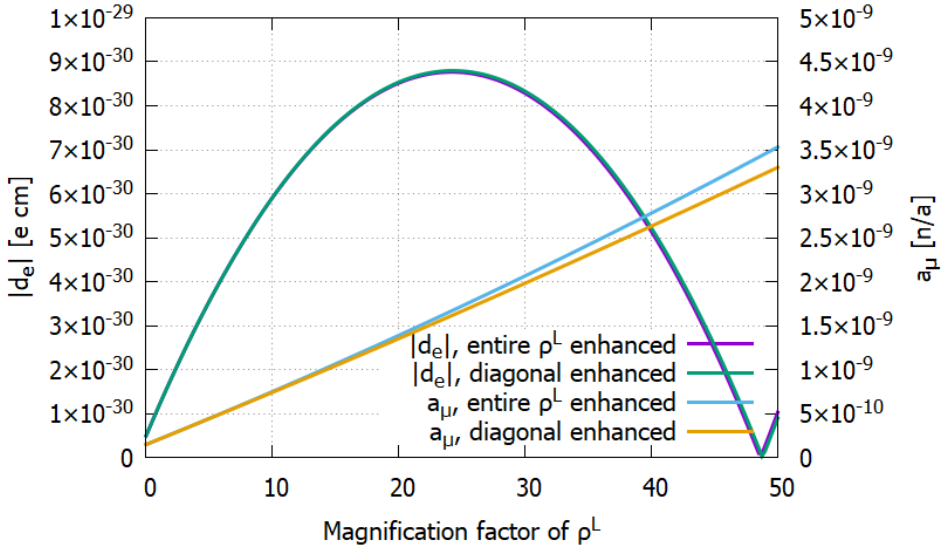

(a) $\arg(\lambda_5) = \pi - 10^{-3}$.

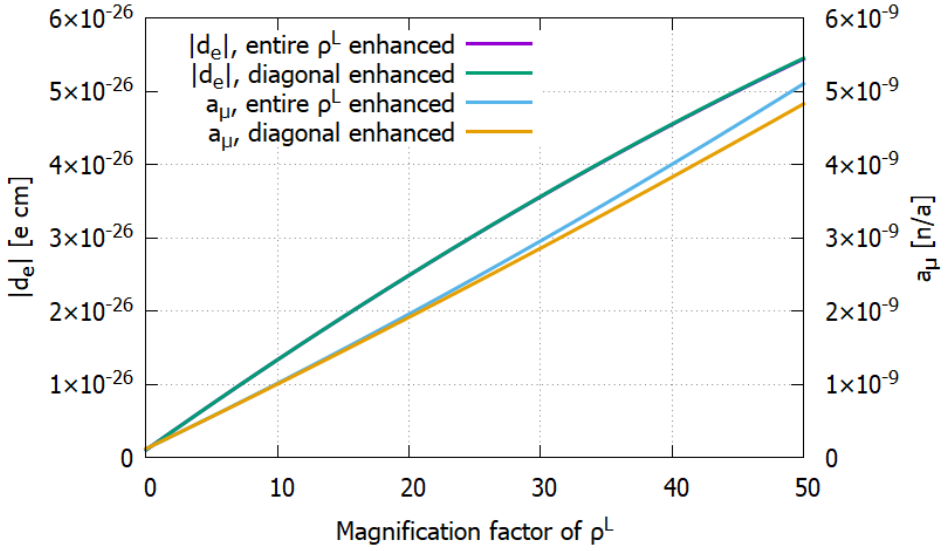

(b) $\arg(\lambda_5) = 0.613$.

Figure 8: Variation of $|d_e|$ and a_μ as functions of ρ^L magnification factor M acting on the diagonal of or the entirety of the matrix for $\mathbf{P_3}$ defined in Table 3, at a minimum (8a) and a maximum (8b) of $|d_e|$ as a function of $\arg(\lambda_5)$.

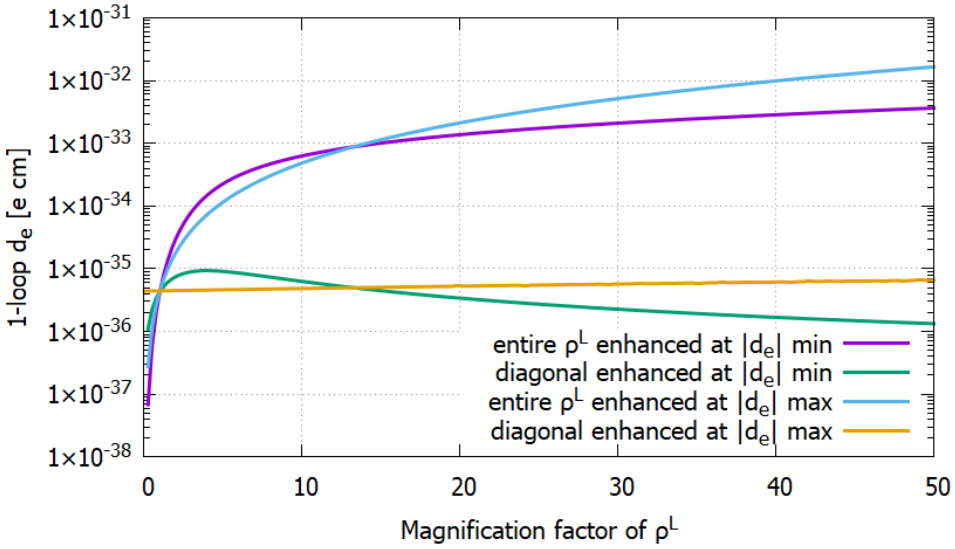

(a) d_e.

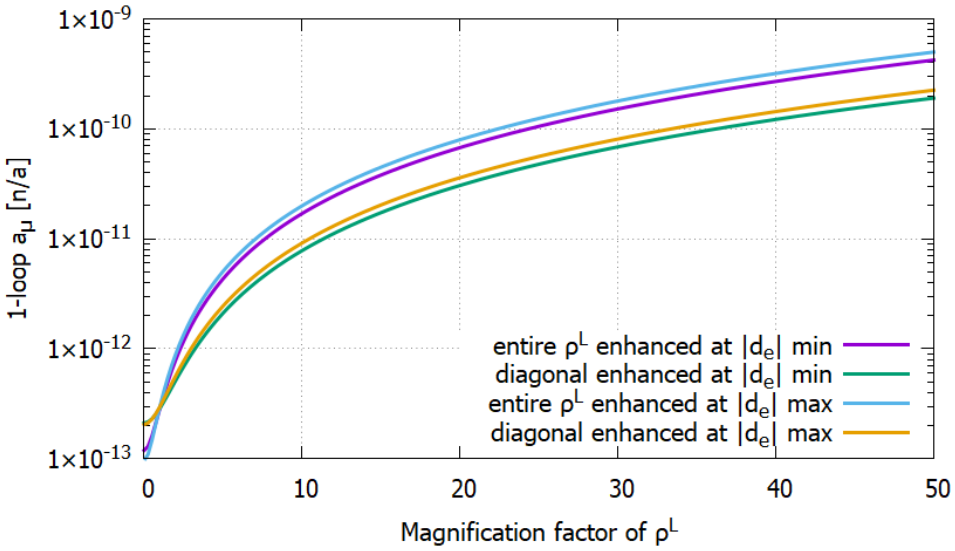

(b) a_μ.

Figure 9: Variation of 1-loop contributions to $|d_e|$ and a_μ as functions of ρ^L magnification factor M acting on the diagonal of or the entirety of the matrix for $\mathbf{P_3}$ defined in Table 3, at a maximum ($\arg(\lambda_5) = 0.613$) and a minimum ($\arg(\lambda_5) = \pi - 10^{-3}$) of $|d_e|$ as a function of $\arg(\lambda_5)$.

4.3 Region III

As there are three independent free complex phases in the scalar potential in this region, phase variation will not be performed here. A two- or three-dimensional parameter study of the effects of phase variation in the potential could be done with an interesting parameter point, such as $\mathbf{P_5}$ (which will soon be detailed), but has not been implemented here. Instead, only the effects of ρ^L magnification, full and diagonal, will be explored. Three 2HDMs, as detailed in Table 4, will be considered. $\mathbf{P_4}$ and $\mathbf{P_5}$ were chosen for providing a sizeable Δa_μ while generating $|d_e|$ within experimental bounds, but $\mathbf{P_5}$ also showed behaviour unseen in any other studied parameter point. $\mathbf{P_6}$ is an arbitrary comparison point. $\mathbf{P_4}$, $\mathbf{P_5}$ and $\mathbf{P_6}$ have ordered neutral scalar boson masses $(121, 241, 367)$ GeV, $(127, 616, 650)$ GeV, and $(125, 581, 659)$ GeV; and charged scalar boson masses 212 GeV, 654 GeV and 587 GeV respectively.

Table 4: The three parameter points studied for region III. The magnification factor M of the ρ^L matrix is allowed to vary freely, while the quark sector is aligned with $a^U = a^D = 1$. The diagonal λ_{ii} elements are equal to 1.

	$\mathbf{P_4}$	$\mathbf{P_5}$	$\mathbf{P_6}$
$\tan\beta$	4.5063	1.1192	2.5273
$\lvert m_{12}^2\rvert$	15616.8	173462	109409
λ_1	0.78562	1.5414	1.9812
λ_2	0.35432	1.5526	0.50552
λ_3	1.4554	1.7128	0.91587
λ_4	1.3952	-1.9812	1.2537
λ_5	$-0.96919 - 1.2518i$	$-0.43759 - 0.45544i$	$-1.2354 + 1.2791i$
λ_6	$0.20632 + 0.12962i$	$-0.06836 + 0.13857i$	$-0.24194 + 0.16732i$
λ_7	$0.15496 + 0.13415i$	$-0.08957 + 0.26120i$	$-0.21459 + 0.01036i$
$\lambda_{e\mu}^L$	0.06101	0.1	0.03657
$\lambda_{e\tau}^L$	0.03278	0.1	0.08586
$\lambda_{\mu e}^L$	0.07280	0.1	0.02384
$\lambda_{\mu\tau}^L$	0.01930	0.1	0.05016
$\lambda_{\tau e}^L$	0.01330	0.1	0.03053
$\lambda_{\tau\mu}^L$	0.08430	0.1	0.02281

$\mathbf{P_4}$ has behaviour largely identical to the points of interest in regions I and II, with d_e cancellation occurring only at an isolated point along the M-axis, as seen in Figure 10a. Just as for $\mathbf{P_1^*}$ in Region II, there is an offset of the $|d_e|$ contribution minima between the fully and diagonally enhanced cases.

Although initially discovered as one of a handful of A2HDMs with a hard $\mathbb{Z}_2$-breaking potential which provided a sizeable Δa_μ while yielding $|d_e|$ within experimental bounds, $\mathbf{P_5}$ also showed $|d_e|$ cancellation for a longer stretch of the M-axis than previously seen

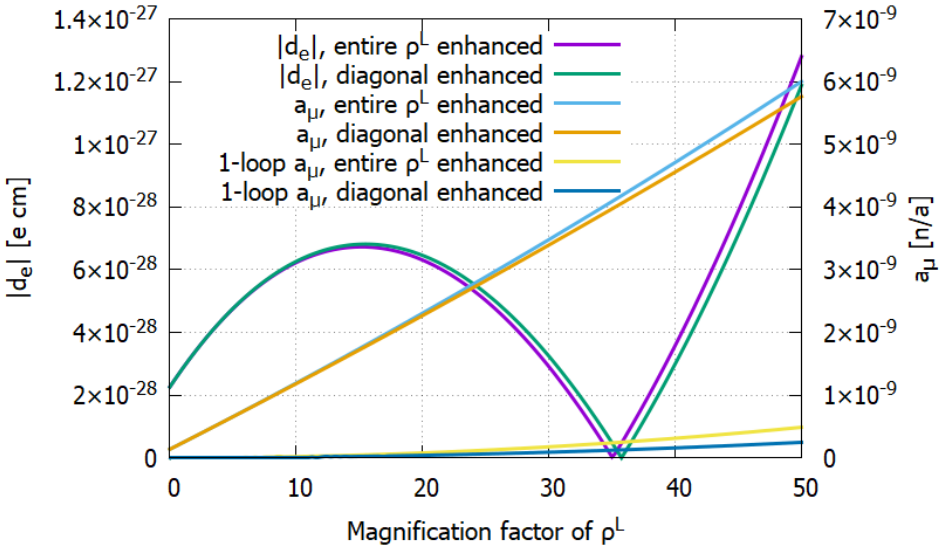

(a) $\mathbf{P_4}$.

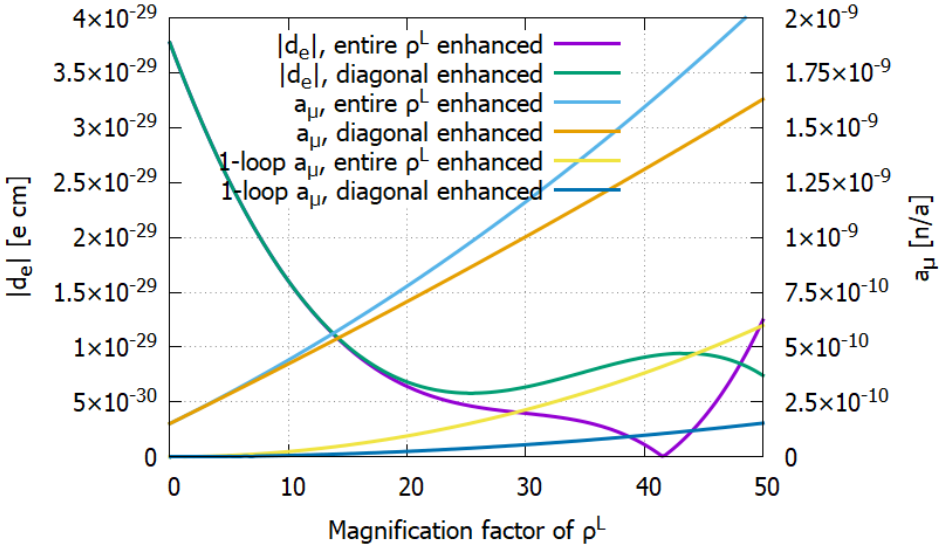

(b) $\mathbf{P_5}$.

Figure 10: Dependence of $|d_e|$ and a_μ on magnification factor for $\mathbf{P_4}$ (10a) and $\mathbf{P_5}$ as defined in Table 4. The magnification factor is a real number M multiplying either the entire ρ^L matrix or just its diagonal elements. $\mathbf{P_5}$ has noticeable d_e cancellation for a large region of the M-interval, unlike $\mathbf{P_4}$ and most other points studied, for which large scale cancellations occur only at isolated points.

in any parameter point upon further study. It was extended to region III by the addition of off-diagonal elements as detailed in Table 4, and d_e cancellation for a long magnitude range remained as Figure 10b shows. Just as $\mathbf{P_1^*}$ evolves identically to $\mathbf{P_1}$ at the resolution and interval provided in the diagonally enhanced case, the diagonally enhanced $\mathbf{P_5}$ evolves identically to the original A2HDM parameter point: If the original parameter point was included in Figure 10b, it would be indistinguishable from the diagonally enhanced $\mathbf{P_5}$. Unlike most points shown, $\mathbf{P_5}$ shows a region of large difference between the diagonally and entirely enhanced cases, where $|d_e|$ has what appears to be a global minimum in the fully enhanced case while it has local maximum in the diagonally enhanced case.

As Figure C.5 shows, $\mathbf{P_6}$ does not have any points or regions d_e cancellation in the interval $M \in [0, 50]$. However, it does show a downwards trend as M gets large, suggesting there may be some point of cancellation for $50 < M$ for both the fully and diagonally enhanced cases.

4.4 Remarks

Although not depicted in any figures, the overall linear nature of a_μ continues to the region of the ρ^L magnification factor $M \in [-50, 0]$. All points studied here give positive values for a_μ at $M = 1$ and have consequently given negative a_μ contributions for the majority of this region. Although unstudied, it may follow that parameter points that give rise to negative a_μ contributions at $M = 1$ would provide remarkable, positive a_μ contributions for large, negative values of M.

A randomly chosen comparison point for region III was discarded, due to exhibiting behaviour similar to $\mathbf{P_4}$, having a point of major d_e cancellation in the interval $M \in [0, 50]$. The M-evolution of $\mathbf{P_6}$ is shown in Figure C.5, and it shows a downwards trend for large M. This suggests isolated points of major 2-loop d_e cancellation, or possibly a sign change, somewhere along the M-axis may be common.

The 1-loop contribution to $|d_e|$ has largely been left out of any figures, as it consistently provides no more than 10^{-4} of the total contribution to $|d_e|$, and typically several orders of magnitude less. At large magnification factors M it may contribute as much as 10^{-32} e cm, as Figure 9 shows, but in these regions the total contribution is typically several orders of magnitude larger than the experimental limit.

5 Conclusions

The 1-loop contributions have usually been ignored in studies of $|d_e|$ and a_μ contributions for the 2HDM, as they are subdominant to the Barr-Zee diagram contributions [42]. For the 1-loop d_e contribution, this does seem to hold true even for very large magnitudes of the ρ^L-matrix. However, in such regions the 1-loop a_μ contributions can account for upwards of 10% of the total a_μ contribution of a given 2HDM. Given that 2HDMs in these regions are capable of explaining Δa_μ by themselves, the 1-loop contributions need to be accounted for when examining the 2HDM as a source of Δa_μ. In studies of unenhanced

or only slightly enhanced Yukawa sectors (for the region $M \leq 10$), however, the 1-loop a_μ contribution can be safely ignored as well.

A 2HDM with a strongly enhanced Yukawa lepton sector could explain the discrepancy between experimental measurements and SM predictions for a_μ. Despite $|d_e|$ contributions growing large in such parameter regions, it has been shown that there may be points or extended regions of the magnification axis where individual 2-loop contributions to $|d_e|$ may cancel out in the sum, predicting a value for $|d_e|$ several orders of magnitude smaller than current experimental limitations while generating an a_μ of the same order of magnitude as Δa_μ. However, these points may still have larger $|d_e|$ contributions from higher order corrections — they may simply be points where the total 2-loop contribution changes sign, which would say very little about the general nature of higher order contributions there — making further analysis necessary.

Potentials with both soft and hard $\mathbb{Z}_2$-violation have been shown to possibly have isolated 2-loop $|d_e|$ minima where large cancellations may occur — the former even in the case of large values for $\mathrm{Im}(\lambda_5)$ — but the latter have also been shown to possibly have extended magnitude regions with small total d_e contributions. There is insufficient data provided by this project to say anything about how common intervals of smaller total $|d_e|$ contributions are, making them an object of possible future studies. One possible area of future study could be 2HDMs with hard $\mathbb{Z}_2$-violating potentials, but $\mathbb{Z}_2$ symmetry applied to the Yukawa sector; such models would eliminate FCNCs at the electroweak scale while limiting the number of free parameters severely.

In the case of 2HDMs with a softly $\mathbb{Z}_2$-violating potential, it is possible to minimise $|d_e|$ while still allowing for some level of $\mathcal{CP}$-violation by requiring a very small, non-zero phase for λ_5 (while setting the phase of m_{12}^2 with the tadpole equations). However, larger amounts of $\mathcal{CP}$-violation are possibly obtained in 2HDMs with a large λ_5 phase at points of 2-loop d_e cancellation, for which higher order contributions have to be analysed. The same conclusions can be said about the potential with hard $\mathbb{Z}_2$-violation, but the phases of $\lambda_{5,6,7}$ must then all be minimised simultaneously.

However, this does not necessarily mean that a 2HDM with a strongly enhanced Yukawa lepton sector is actually viable. Flavour constraints have been kept in mind by treating the enhancement of the entire ρ^L-matrix and only its diagonal separately, as the former quickly reaches regions where FCNCs would be outside of experimental bounds, but other experimental limits have not been considered. Branching ratios and cross sections of the new Higgs bosons may be within experimentally restricted areas for these enhanced regions. The oblique parameters S, T, and U have not been given any consideration either.

It remains to be seen whether analysis of further parameter space restrictions such as those mentioned and others disregarded leave any enhanced Yukawa lepton sector 2HDMs viable. Should they do, the 2HDM is one possibility for explaining Δa_μ and for providing an extra source of $\mathcal{CP}$-violation, which could help solve the problem of baryogenesis. Nevertheless, nothing conclusive can yet be said, but the 2HDM remains a relevant candidate for BSM physics.

Acknowledgements

The utmost gratitude is extended to Johan Rathsman, without whose supervision this project would never have gotten off the ground, not to mention been finished, and to Lukas Esperi, for fruitful and thought-provoking discussion, as well as general support in the writing process.

A 1-loop calculations

As no sources detailing the 1-loop a_μ and d_e contributions of the fully generalised 2HDM were found, these were calculated in the early stages of this project. A `FORM` program [58], based on one made to calculate the SM Higgs contribution to a_μ, was used to determine the vertex terms in Figure 1a. These were in turn used to arrive at the analytic terms for the 1-loop contributions in eq. 9 and 10, which were then compared with references [42, 53] to make sure they reduced to the previously studied results in the A2HDM case.

B Instruction manuals

All three programs detailed are built using the `2HDME` API, available with an installation manual in reference [34]. The source code for this project is available at `https://github.com/zenwet/2hdmSearcher`. Add the `src` folder available there to the `2HDME` repository and overwrite `EDM.cpp` and `EDM.h`. Add `PROG=2hdmSearcher phaseTester magTester` to the Makefile before compiling in order to install the programs.

At this time, the programs are largely undocumented and uncommented, and may be difficult to parse. Effort will be put into remedying this in the near future. They are also error prone, and expect very specific inputs. The modularity is also low.

Functionally, all three programs are very similar. They take take 2HDM potentials and Yukawa sectors (ρ^F-matrices in the Higgs basis) as inputs, and output results in `.dat` format files in the `/output/data` directory.

B.1 `2hdmSearcher`

When run, `2hdmSearcher` will ask whether you want to search for $\mathbb{Z}_2$-symmetric, aligned, or general 2HDMs. In all cases, intervals for $\tan\beta$ and generic potential λ_i and $|m_{12}^2|$ are taken as inputs, with generic potential $|\lambda_i|$ assumed to range from 0 to an input maximum whereas the full interval is taken as input for the other two parameters as well as any complex phases. In the case of aligned 2HDMs, an interval for the alignment parameters a^F is also taken as input, with magnitude and phase intervals taken separately. For a fully general 2HDM search, diagonal and off-diagonal Cheng-Sher parametrisation λ_{ij}^F are given separate intervals (although the diagonal λ_{ii}^F elements will be equal for individual ρ^F-matrices in each 2HDM). A maximum value for $|d_e|$ and a minimum value for a_μ need to be input, as well as the number of random datapoints that are to be searched.

The program outputs two `.dat` format files: One contains all initialised parameter points with lightest neutral scalar boson mass in the region $[120, 130]$ GeV/c, and the other contains the subset of this list which yield $|d_e|$ lower than the input maximum value and a_μ larger than the input minimum value (note the lack of absolute value for a_μ). The outputs contain the potential information for all 2HDMs; their respective λ_{ij}^L for the case of $\mathbb{Z}_2$ symmetry, alignment parameters a^F for the aligned case, or all Cheng-Sher

ansatz λ_{ij}^F parameters for the general case; the Higgs boson masses, as well as $|d_e|$ and a_μ contributions.

Extending `2hdmSearcher` based on the results of this thesis could include searching randomly 2HDMs over a ρ^L magnitude region, rather than just at isolated points, as this could increase the odds of finding isolated cancellation magnitude points such as those shown e.g. in Figure C.2.

B.2 `phaseTester`

`phaseTester` takes a generic basis softly $\mathbb{Z}_2$-violating 2HDM potential, as well as a Higgs basis ρ^L-matrix (in the form of the λ_{ij}^L parameters in the Cheng-Sher ansatz) and varies the phase of λ_5 over the interval $[0, \pi]$, checking total and 1-loop d_e and a_μ at each step and outputting the results into a `.dat` format file, along with the defining information of the given 2HDM. `phaseTester` currently assumes that the Yukawa quark sector is aligned, with alignment factors $a^U = a^D = 1$, as well as a real ρ^L-matrix (although this only applies to the input function — the actual phase-testing function can take arbitrary complex 3×3 matrices as input).

B.3 `magTester`

`magTester` takes a general generic basis 2HDM potential, as well as a Higgs basis ρ^L-matrix (in the form of the λ_{ij}^L parameters in the Cheng-Sher ansatz), and varies the magnitude of either the entire or just the diagonal of the ρ^L-matrix over a (real) user input interval, checking total and 1-loop d_e and a_μ at each step and outputting the results into a `.dat` format file, along with the defining information of the given 2HDM. `magTester` currently assumes that the Yukawa quark sector is aligned, with alignment factors $a^U = a^D = 1$, as well as a real ρ^L-matrix (although this only applies to the input function — the actual phase-testing function can take arbitrary complex 3×3 matrices as input).

C Extra figures

C.1 Region I

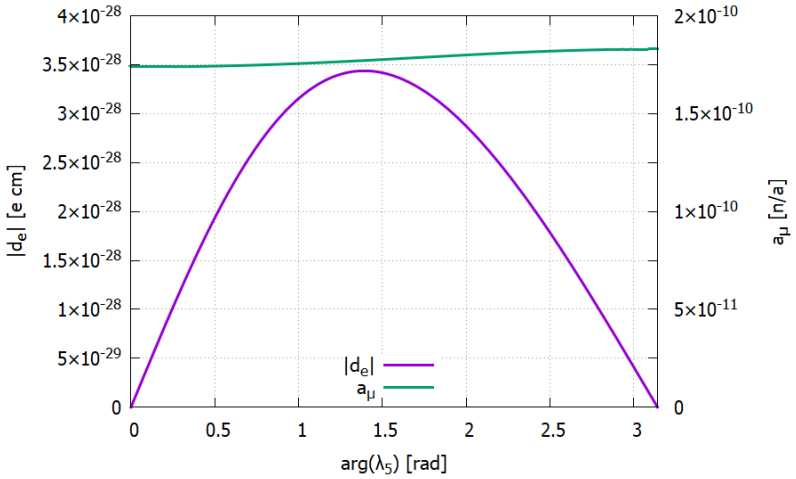

(a) $|d_e|$ and a_μ variation.

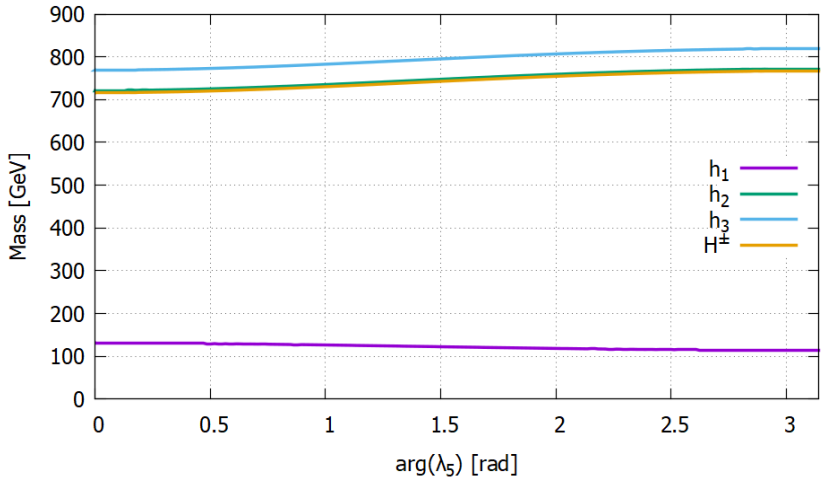

(b) Scalar boson mass variation. h_i denotes a charge neutral boson, while $H^\pm$ denotes a charged boson.

Figure C.1: Variation of $|d_e|$ and a_μ (C.1a) and scalar boson masses (C.1b) with $\arg(\lambda_5)$ for the 2HDM defined at $\mathbf{P_2}$ in Table 2 with $a^L = 1$.

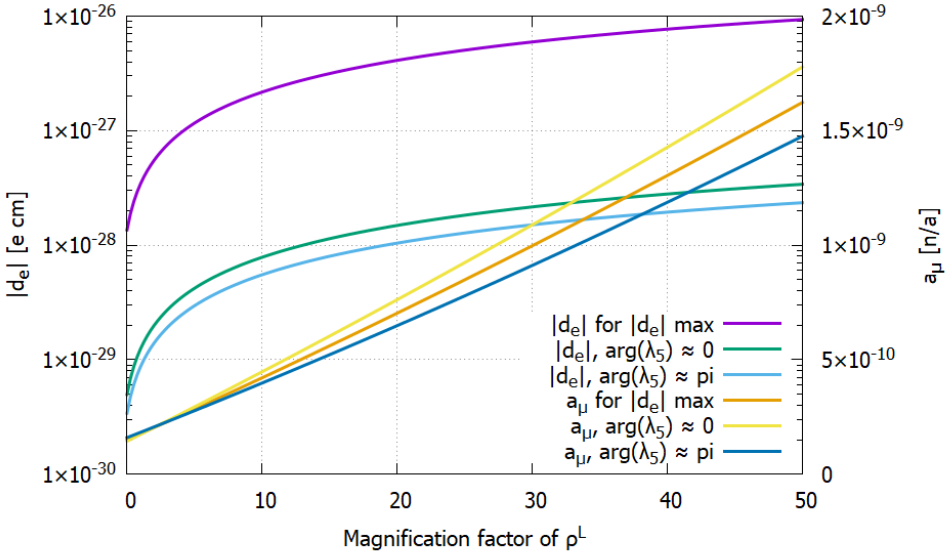

Figure C.2: Variation of $|d_e|$ and a_μ contributions with a^L at $\mathbf{P_2}$ as in Table 2 for the minima and maxima of $|d_e|$ in figure C.1a.

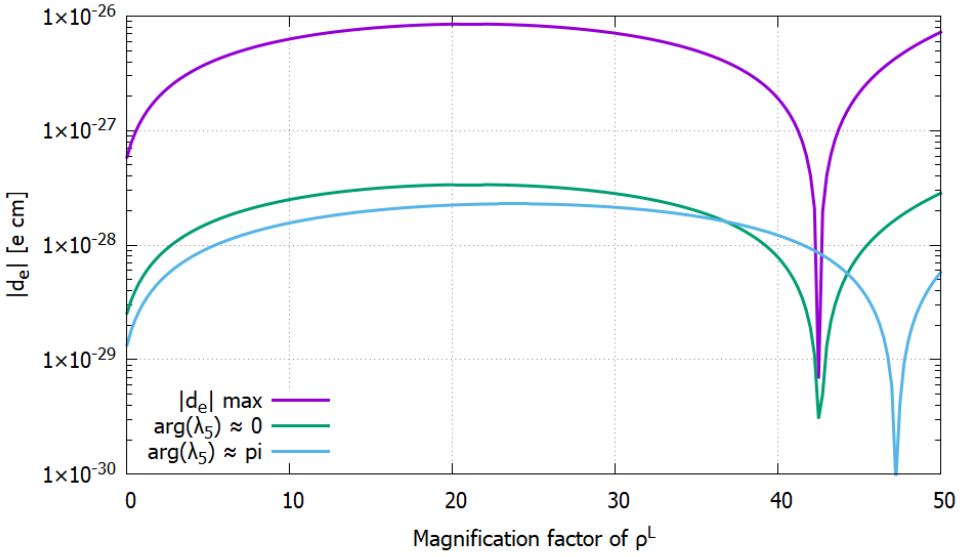

Figure C.3: Variation of $|d_e|$ contributions with a^L at $\mathbf{P_1}$ as in Table 2 for $\arg(\lambda_5) \approx 0$, $\arg(\lambda_5) = 1.34$, and $\arg(\lambda_5) \approx \pi$. Approximately here denotes a deviation of order 10^{-2}.

C.2 Region II

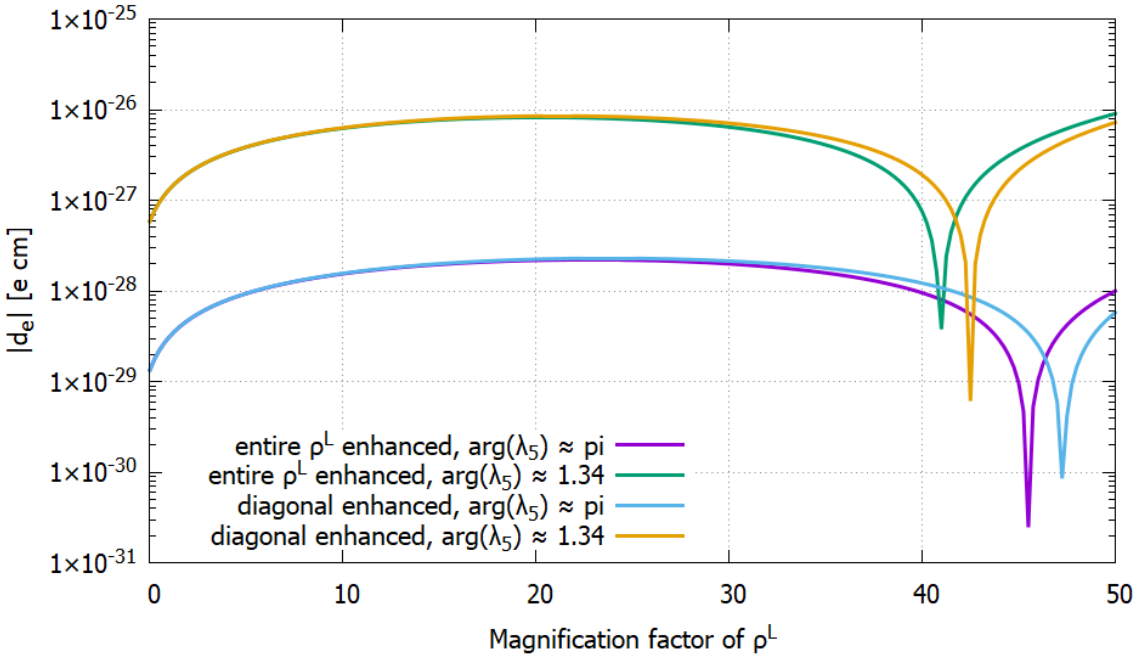

(a) d_e.

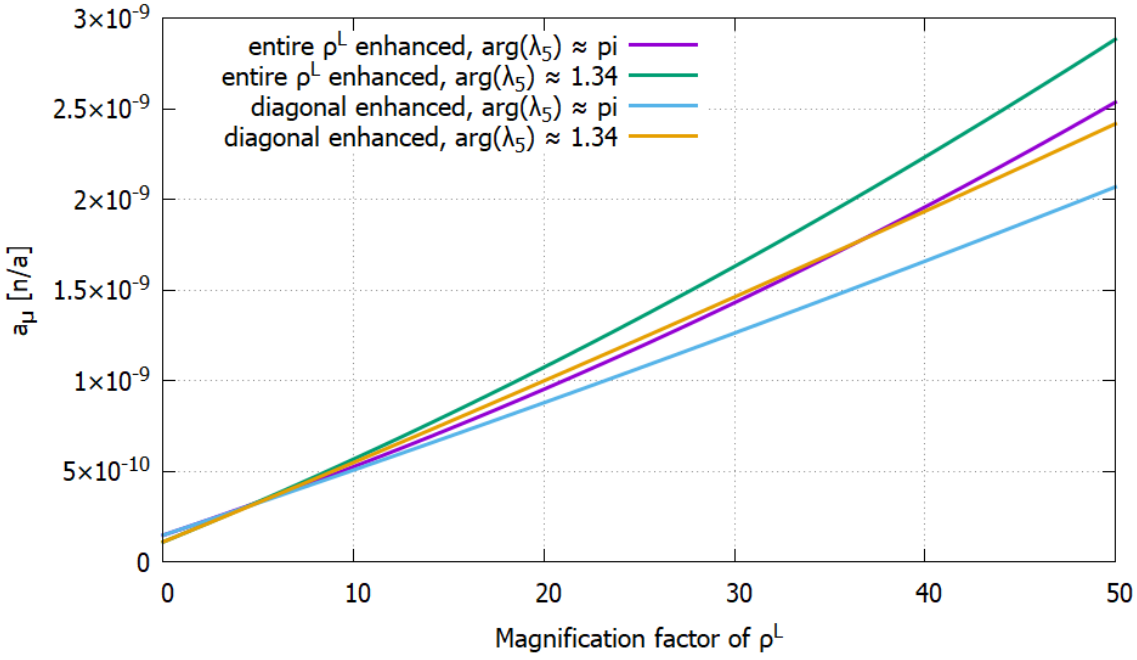

(b) a_μ.

Figure C.4: Evolution of d_e (C.4a) and a_μ (C.4b) with the magnitude factor acting on ρ^L for $\mathbf{P_1^*}$ as defined in Table 3. The magnitude factor is a real number M multiplying either the entire ρ^L matrix or just its diagonal elements. Here, approximately denotes a deviation of order 10^{-3}.

C.3 Region III

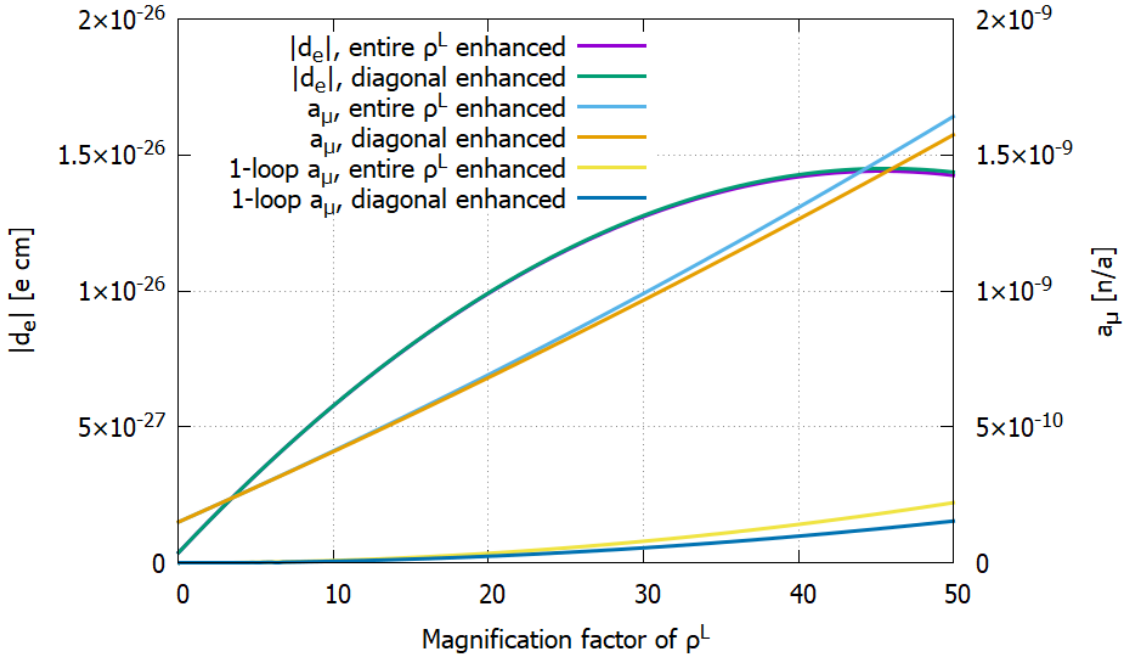

Figure C.5: Evolution of a_μ and $|d_e|$ contributions as functions of magnification factor M acting on the ρ^L-matrix for $\mathbf{P_6}$ as defined in Table 4. M is a real number multiplied with either the entirety of or only the diagonal elements of the ρ^L-matrix.

References

[1] **ATLAS** Collaboration, G. Aad et al. "Observation of a new particle in the search for the Standard Model Higgs boson with the ATLAS detector at the LHC". In: *Phys. Lett.* B716 (2012), pp. 1–29. arXiv: 1207.7214 [hep-ex].

[2] **CMS** Collaboration, S. Chatrchyan et al. "Observation of a new boson at a mass of 125 GeV with the CMS experiment at the LHC". In: *Physics Letters B* 716.1 (2012), pp. 30–61. arXiv: 1207.7235 [hep-ex].

[3] **ATLAS, CMS** Collaboration, G. Aad et al. "Measurements of the Higgs boson production and decay rates and constraints on its couplings from a combined ATLAS and CMS analysis of the LHC pp collision data at $\sqrt{s} = 7$ and 8 TeV". In: *JHEP* 08 (2016), p. 045. arXiv: 1606.02266 [hep-ex].

[4] A. Franklin. "The missing piece of the puzzle: the discovery of the Higgs boson". In: *Synthese* 194.2 (2017), pp. 259–274. DOI: 10.1007/s11229-014-0550-y.

[5] F. Englert and R. Brout. "Broken Symmetry and the Mass of Gauge Vector Mesons". In: *Phys. Rev. Lett.* 13 (9 Aug. 1964), pp. 321–323. DOI: 10.1103/PhysRevLett.13.321.

[6] P. W. Higgs. "Broken Symmetries and the Masses of Gauge Bosons". In: *Phys. Rev. Lett.* 13 (16 Oct. 1964), pp. 508–509. DOI: 10.1103/PhysRevLett.13.508.

[7] G. S. Guralnik, C. R. Hagen and T. W. B. Kibble. "Global Conservation Laws and Massless Particles". In: *Phys. Rev. Lett.* 13 (20 Nov. 1964), pp. 585–587. DOI: 10.1103/PhysRevLett.13.585.

[8] J. Ellis. "Limits of the Standard Model". In: 2002. arXiv: hep-ph/0211168 [hep-ph].

[9] J. Ellis. "Outstanding questions: physics beyond the Standard Model". In: *Phil. Trans. R. Soc. A.* 370 (1961 Feb. 2012), pp. 818–830. DOI: 10.1098/rsta.2011.0452.

[10] CERN. *The Standard Model*. URL: https://home.cern/science/physics/standard-model (visited on 30/04/2020).

[11] J. Barranco. "Some Standard model problems and possible solutions". In: *Journal of Physics: Conference Series* 761 (Oct. 2016), p. 012007. DOI: 10.1088/1742-6596/761/1/012007.

[12] A. D. Sakharov. "Violation of CP Invariance, C Asymmetry, and Baryon Asymmetry of the Universe". In: *JETP Lett.* 5.1 (1967), pp. 24–27. URL: http://www.jetpletters.ac.ru/ps/1643/article_25089.shtml.

[13] M. J. Duff. *A Layman's Guide to M-theory*. 1998. arXiv: hep-th/9805177 [hep-th].

[14] J. F. Gunion et al. *The Higgs Hunter's Guide*. Frontiers in Physics, 80. Perseus Books, 2000. ISBN: 978-0-738-20305-8.

[15] L. Fromme, S. J. Huber and M. Seniuch. "Baryogenesis in the two-Higgs doublet model". In: *Journal of High Energy Physics* 2006.11 (Nov. 2006), p. 038. ISSN: 1029-8479. DOI: 10.1088/1126-6708/2006/11/038. arXiv: hep-ph/0605242 [hep-ph].

[16] H. E. Haber and G. L. Kane. "The search for supersymmetry: Probing physics beyond the standard model". In: *Physics Reports* 117.2 (1985), pp. 75–263. ISSN: 0370-1573. DOI: https://doi.org/10.1016/0370-1573(85)90051-1. URL: http://www.sciencedirect.com/science/article/pii/0370157385900511.

[17] ATLAS Experiment. *New searches for supersymmetry presented by ATLAS experiment*. 19 May 2019. URL: https://phys.org/news/2019-05-supersymmetry-atlas.html (visited on 02/05/2020).

[18] J. E. Kim. "Light Pseudoscalars, Particle Physics and Cosmology". In: *Phys. Rept.* 150 (1987), pp. 1–177. DOI: 10.1016/0370-1573(87)90017-2.

[19] E. O. Iltan and H. Sundu. "Anomalous magnetic moment of the muon in the two Higgs doublet model". In: (2001). arXiv: hep-ph/0103105 [hep-ph].

[20] **Particle Data Group** Collaboration, M. Tanabishi et al. In: *Phys. Rev. D* 98 (3 Aug. 2018), p. 030001. DOI: 10.1103/PhysRevD.98.030001.

[21] M. Davier et al. "Hadron Contribution to Vacuum Polarisation". In: vol. 26. 2016. Chap. 7, pp. 129–144. DOI: 10.1142/9789814733519_0007.

[22] E. J. Chun, J. Kim and T. Mondal. "Electron EDM and Muon anomalous magnetic moment in Two-Higgs-Doublet Models". In: *Journal of High Energy Physics* 2019.12 (Dec. 2019). ISSN: 1029-8479. DOI: 10.1007/jhep12(2019)068. arXiv: 1906.00612 [hep-ph].

[23] **ACME** Collaboration, V. Andreev et al. "Improved limit on the electric dipole moment of the electron". In: *Nature* 562 (Oct. 2018), pp. 355–360. DOI: 10.1038/s41586-018-0599-8.

[24] G. C. Branco et al. "Theory and phenomenology of two-Higgs-doublet models". In: *Physics Reports* 516.1-2 (July 2012), pp. 1–102. ISSN: 0370-1573. DOI: 10.1016/j.physrep.2012.02.002. arXiv: 1106.0034 [hep-ph].

[25] P. Langacker. "Grand unified theories and proton decay". In: *Physics Reports* 72.4 (1981), pp. 185–385. ISSN: 0370-1573. DOI: https://doi.org/10.1016/0370-1573(81)90059-4.

[26] J. Oredsson. "Soft resummation and hard evolution. Renormalization group methods in effective theories and multi scalar models". PhD thesis. Lund University, 2019. ISBN: 978-91-7895-255-7.

[27] G. C. Branco, L. Lavoura and J. P. Silva. *CP Violation*. 1st. International Series of Monographs on Physics. Oxford University Press, 1999. ISBN: 978-0-198-50399-6.

[28] H. E. Haber and D. O'Neil. "Basis-independent methods for the two-Higgs-doublet model. II. The significance of $\tan\beta$". In: *Physical Review D* 74.1 (July 2006). ISSN: 1550-2368. DOI: 10.1103/physrevd.74.015018. arXiv: hep-ph/0602242 [hep-ph]. URL: http://dx.doi.org/10.1103/PhysRevD.74.015018.

[29] S. Davidson and H. E. Haber. "Basis-independent methods for the two-Higgs-doublet model". In: *Phys. Rev. D* 72 (2005). [Erratum: Phys.Rev.D 72, 099902 (2005)], p. 035004. DOI: 10.1103/PhysRevD.72.099902. arXiv: hep-ph/0504050.

[30] T. P. Cheng and M. Sher. "Mass Matrix Ansatz and Flavor Nonconservation in Models with Multiple Higgs Doublets". In: *Phys. Rev. D* 35 (1987), p. 3484. DOI: 10.1103/PhysRevD.35.3484.

[31] J. Bijnens, J. Lu and J. Rathsman. "Constraining general two Higgs doublet models by the evolution of Yukawa couplings". In: *Journal of High Energy Physics* 2012.5 (May 2012). ISSN: 1029-8479. DOI: 10.1007/jhep05(2012)118. arXiv: 1111.5760 [hep-ph].

[32] J. L. Diaz-Cruz, R. Noriega-Papaqui and A. Rosado. "Mass matrix ansatz and lepton flavor violation in the THDM-III". In: *Phys. Rev. D* 69 (2004), p. 095002. DOI: 10.1103/PhysRevD.69.095002. arXiv: hep-ph/0401194.

[33] M. E. Krauss and F. Staub. "Perturbativity constraints in BSM models". In: *The European Physical Journal C* 78.3 (Mar. 2018). ISSN: 1434-6052. DOI: 10.1140/epjc/s10052-018-5676-5. arXiv: 1709.03501 [hep-ph].

[34] J. Oredsson. "2HDME: Two-Higgs-Doublet Model Evolver". In: *Computer Physics Communications* 244 (Nov. 2019), pp. 409–426. ISSN: 0010-4655. DOI: 10.1016/j.cpc.2019.05.021. arXiv: 1811.08215 [hep-ph]. URL: https://github.com/jojelen/2HDME.

[35] I. F. Ginzburg and I. P. Ivanov. "Tree-level unitarity constraints in the most general two Higgs doublet model". In: *Physical Review D* 72.11 (Dec. 2005). ISSN: 1550-2368. DOI: 10.1103/physrevd.72.115010. arXiv: hep-ph/0508020 [hep-ph].

[36] M. D. Goodsell and F. Staub. "Improved unitarity constraints in Two-Higgs-Doublet-Models". In: *Physics Letters B* 788 (Jan. 2019), pp. 206–212. ISSN: 0370-2693. DOI: 10.1016/j.physletb.2018.11.030. arXiv: 1805.07310 [hep-ph].

[37] I. P. Ivanov. "Minkowski space structure of the Higgs potential in 2HDM". In: *Phys. Rev. D* 75 (2007). [Erratum: Phys.Rev.D 76, 039902 (2007)], p. 035001. DOI: 10.1103/PhysRevD.75.035001. arXiv: hep-ph/0609018 [hep-ph].

[38] I. P. Ivanov. "Minkowski space structure of the Higgs potential in 2HDM. II. Minima, symmetries, and topology". In: *Phys. Rev. D* 77 (2008), p. 015017. DOI: 10.1103/PhysRevD.77.015017. arXiv: 0710.3490 [hep-ph].

[39] F. Staub. "Reopen parameter regions in two-Higgs doublet models". In: *Physics Letters B* 776 (Jan. 2018), pp. 407–411. ISSN: 0370-2693. DOI: 10.1016/j.physletb.2017.11.065. arXiv: 1705.03677 [hep-ph].

[40] C. J. Foot. *Atomic Physics*. 1st ed. Oxford master series in physics 7. Atomic, Optical, and laser physics. Oxford University Press, 2005. ISBN: 978-0-198-50696-6.

[41] T. Aoyama, T. Kinoshita and M. Nio. "Theory of the Anomalous Magnetic Moment of the Electron". In: *Atoms* 7.1 (2019), p. 28. DOI: 10.3390/atoms7010028.

[42] V. Ilisie. "New Barr-Zee contributions to ($g2$) in two-Higgs-doublet models". In: *Journal of High Energy Physics* 2015.4 (Apr. 2015). ISSN: 1029-8479. DOI: 10.1007/jhep04(2015)077. arXiv: 1502.04199 [hep-ph].

[43] M. Pospelov and A. Ritz. "Electric dipole moments as probes of new physics". In: *Annals of Physics* 318.1 (July 2005), pp. 119–169. ISSN: 0003-4916. DOI: 10.1016/j.aop.2005.04.002. arXiv: hep-ph/0504231 [hep-ph].

[44] D. Ghosh and R. Sato. "Lepton electric dipole moment and strong CP violation". In: *Physics Letters B* 777 (Feb. 2018), pp. 335–339. ISSN: 0370-2693. DOI: 10.1016/j.physletb.2017.12.052. arXiv: 1709.05866 [hep-ph].

[45] M. Jung and A. Pich. "Electric dipole moments in two-Higgs-doublet models". In: *Journal of High Energy Physics* 2014.4 (Apr. 2014). ISSN: 1029-8479. DOI: 10.1007/jhep04(2014)076. arXiv: 1308.6283 [hep-ph].

[46] S. Ipek. "Perturbative analysis of the electron electric dipole moment and CP violation in two-Higgs-doublet models". In: *Physical Review D* 89.7 (Apr. 2014). ISSN: 1550-2368. DOI: 10.1103/physrevd.89.073012. arXiv: 1310.6790 [hep-ph].

[47] L. Bian, T. Liu and J. Shu. "Cancellations Between Two-Loop Contributions to the Electron Electric Dipole Moment with a CP-Violating Higgs Sector". In: *Physical Review Letters* 115.2 (July 2015). ISSN: 1079-7114. DOI: 10.1103/physrevlett.115.021801. arXiv: 1411.6695 [hep-ph].

[48] D. Egana-Ugrinovic and S. Thomas. "Higgs Boson Contributions to the Electron Electric Dipole Moment". In: (Oct. 2018). arXiv: 1810.08631 [hep-ph].

[49] J. Oredsson and J. Rathsman. "2-loop RG evolution of $\mathcal{CP}$-violating 2HDM". In: (Sept. 2019). arXiv: 1909.05735 [hep-ph].

[50] A. Pich and P. Tuzón. "Yukawa alignment in the two-Higgs-doublet model". In: *Physical Review D* 80.9 (Nov. 2009). ISSN: 1550-2368. DOI: 10.1103/physrevd.80.091702. arXiv: 0908.1554 [hep-ph].

[51] I. F. Ginzburg and M. Krawczyk. "Symmetries of two Higgs doublet model and CP violation". In: *Physical Review D* 72.11 (Dec. 2005). ISSN: 1550-2368. DOI: 10.1103/physrevd.72.115013. arXiv: hep-ph/0408011 [hep-ph].

[52] I. Chakraborty and A. Kundu. "Scalar potential of two-Higgs doublet models". In: *Physical Review D* 92.9 (Nov. 2015). ISSN: 1550-2368. DOI: 10.1103/physrevd.92.095023. arXiv: 1508.00702 [hep-ph].

[53] V. Keus, N. Koivunen and K. Tuominen. "Singlet scalar and 2HDM extensions of the Standard Model: CP-violation and constraints from $(g-2)_\mu$ and eEDM". In: *Journal of High Energy Physics* 2018.9 (Sept. 2018). ISSN: 1029-8479. DOI: 10.1007/jhep09(2018)059. arXiv: 1712.09613 [hep-ph].

[54] J. Oredsson and J. Rathsman. "$\mathbb{Z}_2$ breaking effects in 2-loop RG evolution of 2HDM". In: *Journal of High Energy Physics* 2019.2 (Feb. 2019). ISSN: 1029-8479. DOI: 10.1007/jhep02(2019)152. arXiv: 1810.02588 [hep-ph].

[55] S. M. Barr and A. Zee. "Electric Dipole Moment of the Electron and of the Neutron". In: *Phys. Rev. Lett.* 65 (1990). [Erratum: Phys.Rev.Lett. 65, 2920 (1990)], pp. 21–24. DOI: 10.1103/PhysRevLett.65.21.

[56] D. Chang, W.-Y. Keung and T. C. Yuan. "Two loop bosonic contribution to the electron electric dipole moment". In: *Phys. Rev. D* 43 (1991), pp. 14–16. DOI: 10.1103/PhysRevD.43.R14.

[57] S. Inoue, M. J. Ramsey-Musolf and Y. Zhang. "CP-violating phenomenology of flavor conserving two Higgs doublet models". In: *Phys. Rev. D* 89.11 (2014), p. 115023. DOI: 10.1103/PhysRevD.89.115023. arXiv: 1403.4257 [hep-ph].

[58] B. Ruijl, T. Ueda and J. Vermaseren. *FORM version 4.2*. July 2017. arXiv: 1707.06453 [hep-ph].